

pH sensitive functionalized hyperbranched polyester based nanoparticulate system for the receptor-mediated targeted cancer therapy

Ayça Bal Öztürk, Erdal Cevher, Serhat Pabuccuoğlu & Saadet Özgümüş

To cite this article: Ayça Bal Öztürk, Erdal Cevher, Serhat Pabuccuoğlu & Saadet Özgümüş (2018): pH sensitive functionalized hyperbranched polyester based nanoparticulate system for the receptor-mediated targeted cancer therapy, International Journal of Polymeric Materials and Polymeric Biomaterials, DOI: [10.1080/00914037.2018.1452226](https://doi.org/10.1080/00914037.2018.1452226)

To link to this article: <https://doi.org/10.1080/00914037.2018.1452226>



Published online: 04 Apr 2018.



Submit your article to this journal [↗](#)



Article views: 17



View related articles [↗](#)



View Crossmark data [↗](#)

pH sensitive functionalized hyperbranched polyester based nanoparticulate system for the receptor-mediated targeted cancer therapy

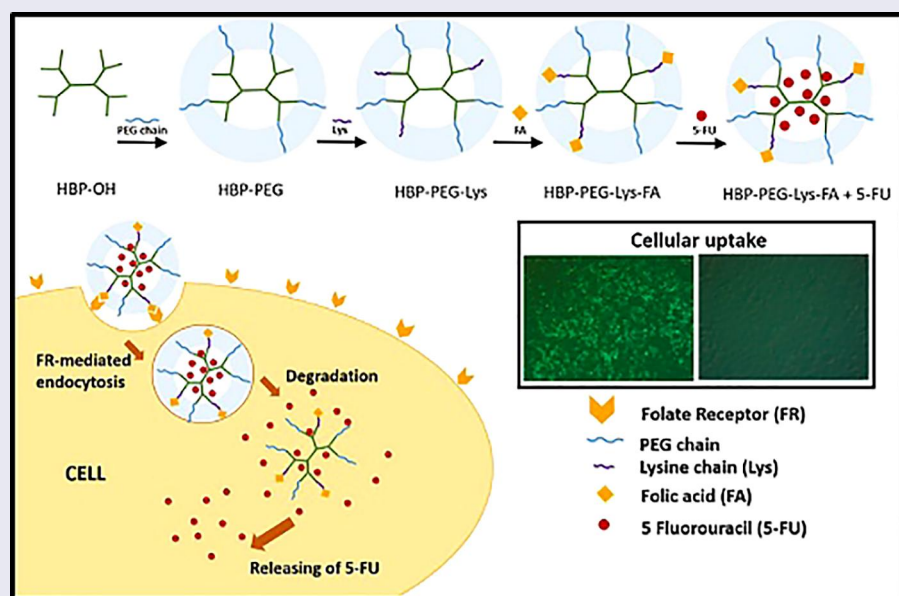
Ayça Bal Öztürk^a, Erdal Cevher^b, Serhat Pabuccuoğlu^c and Saadet Özgümüş^a

^aDepartment of Chemical Engineering, Faculty of Engineering, Istanbul University, Istanbul, Turkey; ^bDepartment of Pharmaceutical Technology, Faculty of Pharmacy, Istanbul University, Istanbul, Turkey; ^cDepartment of Reproduction and Artificial Insemination, Faculty of Veterinary Medicine, Istanbul University, Istanbul, Turkey

ABSTRACT

The aim of this study is to develop a novel folic acid conjugated, DL-lysine modified, PEGylated, the 3rd generation hyperbranched polymer (HBP-PEG-Lys-FA) for use in receptor-mediated therapy. 5-fluorouracil, model anti-cancer drug, loaded nanoparticles were found an average size of 177 nm with loading efficiency of 23.18%. *In vitro* drug release studies demonstrated that nanoparticles showed pH-dependent release. HBP-PEG-Lys-FA were efficiently taken up by HeLa cells and specificity of targeted nanoparticles to folate receptors of cells was proved. It was concluded that the HBP-PEG-Lys-FA nanoparticles can provide an advantage on delivering of the drug efficiently into the cytosol for cancer therapy.

GRAPHICAL ABSTRACT



ARTICLE HISTORY

Received 4 February 2018
Accepted 11 March 2018

KEYWORDS

5-fluorouracil; cancer therapy; hyperbranched polyester; pH sensitive nanoparticles; receptor-mediated targeting; targeted drug carrier

1. Introduction

Cancer is a multiple disease characterized by continuous cell growth and division due to the genetic and environmental changes. Over the past several decades significant improvements have been made in understanding cancer biology. However, cancer still remains one of the leading causes of death worldwide. In particular, most widely used chemotherapeutic drugs are far from perfect with their wide distribution in both healthy and cancerous tissues, which causes undesirable side effects.^[1-3] Extending patients' survival time and improving their quality of life by destroying tumors without damaging

the surrounding healthy tissues are indispensable key factors on effective cancer therapy regime.^[4,5] Targeted nanoparticulate drug delivery systems can provide selective and specific treatment as current cancer treatments based on chemotherapy have serious side-effects related to non-specific uptake of the drug by healthy cells.^[2,3] Nanoparticles offer the advantages of decreased drug toxicity, enhanced drug accumulation at tumor sites *via* passive and active targeting, triggered drug release with environmental stimuli like heat and pH changes.^[6-11] The potential ability of nanoparticles to circulate in the bloodstream for a prolonged period of time is often a prerequisite for the

successful cancer therapy.^[12] Otherwise, nanoparticles depending on their surface characteristics are rapidly recognized and captured by the Mononuclear Phagocytic System (MPS) in bloodstream within seconds or minutes after intravenous injection and rapidly cleared from circulation.^[13,14] To address these limitations and designate the long-circulated nanoparticles, surface modification of the nanoparticles with hydrophilic polymers such as poly(ethylene glycol) (PEG) has emerged as a strategy to reduce their binding capacity to opsonins, the advantages of which reduce opsonization and uptake by MPS, provide relatively long plasma residence time and thus can enhance the potential targetability of the system.^[12,15,16] These carrier systems show an improved extravasation profile with enhanced localization in tumors.^[15]

Active and passive targeting strategies result in a considerable accumulation of the long-circulating nanoparticles at the tumor site, but their anti-cancer efficacy can still be limited because of inadequate drug release in tumor cells.^[17] Efficient cytoplasmic delivery of these drugs is especially important for elicitation of a maximal therapeutic effect.^[18] To address this limitation for an effective cancer therapy, after the cellular internalization of nanoparticles in the endosomal (pH 5-5.5) and lysosomal compartments, anticancer drug loaded nanoparticles are required to be degraded and thus anti-cancer drug within the nanoparticles escape from endosome into the cytosol *via* disrupting the endosomal membrane through proton sponge effect.^[19] Another problem is associated with P-glycoprotein, a multidrug resistance protein that is overexpressed on the surface of the tumor cells, which prevents drug accumulation inside the tumor, acting as the efflux pump, and often mediates the development of resistance to anticancer drugs.^[20] For this reason, drug-loaded nanoparticles should be as stable as possible in blood stream (pH 7.4) and anti-cancer drug from nanoparticles should be quickly released in late endosomes (pH 5-5.5) after the internalization of the drug loaded nanoparticles. For this purpose, nanoparticles sensitive to the pH gradients are promising for cancer drug delivery and several pioneering researchers have been working on pH-sensitive polymeric systems for the effective delivery of anti-cancer drugs to tumors.^[20-22]

Variety of nanoparticles including polymeric, ceramic, metallic based ones, micelles, liposomes, carbon nanotubes and dendrimers have been evaluated in cancer research.^[4] Recent research efforts have been directed towards the possible use of hyperbranched and functionalized polymers, in development of efficient drug carrier systems due to their unique features such as low viscosity, high solubility, plenty of terminal groups and lack of chain entanglements.^[23,24] Hyperbranched polymers have similar configuration with dendrimers but are more easily synthesized than dendrimers.^[25-27] In addition, end-groups of hyperbranched polymers can be easily modified to arrange their solubility, compatibility, reactivity, adhesibility to specific surfaces, self-assemblability and chemical recognizability.^[28]

In this work, a novel folic acid (FA) conjugated, DL-lysine modified, PEGylated, third generation aliphatic-polyester based hyperbranched polymer (HBP-PEG-Lys-FA) was synthesized and after characterization studies, a long circulating and actively targeted nanoparticles containing

model anti-cancer drug, 5-fluorouracil (5-Fu), to folate receptors were fabricated with polymer synthesized. In order to improve their plasma stability and blood circulation time, hyperbranched polymer (HBP) was pegylated^[29] and then the obtained HBP-PEG was modified with DL-lysine (HBP-PEG-Lys) to modify the surface charge of the nanoparticles^[30] and finally FA was conjugated (HBP-PEG-Lys-FA) to enhance intracellular transport of 5-Fu loaded nanoparticles through folate receptor-mediated endocytosis.^[31] Size, zeta potential, serum stability and *in vitro* drug release characteristics of the nanoparticles were determined. Cellular uptake, receptor specificity and cytotoxicity of nanoparticles were evaluated on human cervical carcinoma cells (HeLa).

2. Experimental

2.1. Materials

2,2-bis(hydroxymethyl)propionic acid (Bis-MPA), poly(ethylene glycol) methyl ether (MPEG, Mw ~ 2000Da), maleic anhydride (MA), p-toluenesulfonic acid (p-TSA), DL-lysine monohydrochloride (DL-Lys), di-tert-butyl dicarbonate (BOC₂O), folic acid (FA), N-(3-Dimethylaminopropyl)-N'-ethylcarbodiimide hydrochloride (EDAC), 3-[4,5-dimethylthiazol-2-yl]-2,5-diphenyltetrazolium bromide (MTT) and calcein were purchased from Sigma Aldrich (St. Louis, MO, USA). 4-(Dimethylamino)pyridine (DMAP) and all solvents were acquired from Merck Chemicals Ltd (Hohenbrunn, Germany). Ethoxylated trimethylolpropane (Et-TMP, M_n ~ 170) and 5-Fluorouracil (5-Fu), were gifts of Perstorp Polyols AB, Sweden and Koçak Pharma, Turkey, respectively. Regenerated cellulose membrane dialysis tubing with Mw cut-off of 12-14 kDa were purchased from Sigma Aldrich (St. Louis, MO, USA), respectively. HeLa cells were supplied by the American Type Culture Collection (ATCC), USA. Fetal bovine serum (FBS) and Dulbecco's modified Eagle's medium (DMEM) were purchased from GIBCO (Gaithersburg, MD, USA). All the other reagents were of analytical grade and were used directly without any further purification.

2.2. Synthesis of hydroxyl-terminated hyperbranched polymer (HBP-OH)

HBP-OH was synthesized according to the pseudo-one-step procedure.^[32] Briefly, 6.707 g Bis-MPA (50.0 mmol, repeating unit; in stoichiometric correspondence to the second generation), 0.944 g Et-TMP (5.55 mmol) and a catalytic amount of p-TSA (0.5% of AB₂ type monomer weight) were firstly added into a three-necked cylindrical glass reaction system equipped with a Dean-Stark apparatus, nitrogen gas inlet-outlet and mechanical stirrer system. The reaction system was placed in a pre-heated oil bath at 140°C. After the mixture was reacted for 2.5 h at the same temperature in nitrogen gas atmosphere, 8.933 g Bis-MPA (66.6 mmol, in stoichiometric correspondence to the third generation) and a catalytic amount of p-TSA (0.5% of AB₂ type monomer weight) was added to this mixture. The reaction was monitored at regular time intervals by the determination of the acid value (AV) via a titration method^[32] in which the sample was dissolved in

acetone and titrated with 0.1 N methanolic KOH solution and was allowed to continue until the AV of reaction mixture was below 30 (~5 h). For the purification of HBP-OH, the reaction mixture was dissolved in acetone, precipitated into cold hexane and dried at 25°C in a vacuum. After the purification process, white-colored sticky solid products in high yields (>99%) were obtained. Then, fractional precipitation was applied to HBP-OH to remove the low molecular weight and insoluble fraction. Firstly, HBP-OH was dissolved in acetone and ethyl ether was slowly added to the polymer solution under vigorous mixing. After 12 h, precipitated product was filtered, washed twice with a mixture of acetone/ether (1:1 v/v) and dried at 25°C in a vacuum.

2.3. Synthesis of PEGylated HBP (HBP-PEG)

First, carboxylic acid-terminated PEG (PEG-COOH) was synthesized by the ring-opening reaction of maleic anhydride.^[33] Then, the obtained PEG-COOH (2.1 g, 1 mmol) and HBP-OH (0.22 g, theoretically [OH] = 2 mmol) were dissolved in 20 mL of DMSO and 0.211 g EDAC (1.1 mmol) was added under vigorous stirring at room temperature. After 24 h, 0.122 g DMAP (1 mmol) was added and the stirring was continued overnight. The resulting solution was diluted with deionized water and purified by dialysis (12–14 kDa, Sigma Aldrich, USA) against deionized water using dialysis tubing at room temperature for 3 days and finally lyophilized (Virtis Advantage, SP Scientific, Suffolk, UK). White-coloured HBP-PEG was obtained with a yield of 65%.

2.4. Synthesis of lysine conjugated HBP-PEG (HBP-PEG-Lys)

HBP-PEG-Lys was synthesized by reacting the hydroxyl groups of HBP-PEG with the carboxyl end group of the N-Boc protected DL-Lys in the presence of EDAC and DMAP as the catalysts. Firstly, the α - and ε - amino group of DL-Lys was protected with BOC₂O.^[34] Then, the obtained DL-Lys-BOC (0.29 g, 1 mmol) was treated with EDAC (0.211 g, 1.1 mmol) for 1 h and 1 g HBP-PEG (0.036 mmol) dissolved in 9 mL of deionized water was added to the mixture. After 24 h, 32.1 mg DMAP (0.26 mmol) was added, the stirring was continued overnight, and then purified by dialysis against deionized water at room temperature for 24 h and subsequently lyophilized. BOC groups in HBP-PEG-Lys was deprotected following method.^[35] Briefly, HBP-PEG-Lys-BOC was treated with 4 M HCl/dioxane solution at 0°C in an inert atmosphere and stirred at room temperature for 30 min. The reaction mixture was finally purified as described in the Section 2.3. White-coloured HBP-PEG-Lys was obtained with a yield of 53%.

2.5. Conjugation of FA ligand to HBP-PEG-Lys

Solution of 1 g HBP-PEG-Lys (0.035 mmol) in 6 mL DMSO was treated with 0.013 g EDAC (0.069 mmol) at room temperature in an inert atmosphere for 1 h. Then, 0.046 g FA (0.1 mmol) dissolved in DMSO was added to solution. After proceeding of the reaction for 24 h with stirring at room

temperature, 0.42 mg DMAP (3.46×10^{-3} mmol) was added and allowed to react overnight. Subsequently the reaction mixture was purified as described in Section 2.3 to obtain the yellowish HBP-PEG-Lys-FA in a powder form with a yield of 92% and kept at 4°C until further use.

2.6. Structural characterization of hyperbranched HBP-PEG-Lys-FA polymer

Fourier transform infrared (FT-IR) spectrum of the polymer synthesized (HB-PEG-Lys-FA) was measured in potassium bromide disks (sample/KBr = 1/200) using Digilab Excalibur-FTS 3000 MX model FT-IR spectrometer (USA) in the range of 4000–600 cm⁻¹. ¹H-NMR and ¹³C-NMR spectra were recorded on a Varian UNITY INOVA spectrometer (USA) operating at 500 MHz using CDCl₃ and DMSO (d₆) as the solvents at 25°C.

2.7. pH dependent degradation studies

Polymer degradation studies were performed both in pH 5.5 acetate buffer solution (endosomal pH) and in pH 7.4 phosphate buffer saline (physiological pH). 50 mg of HBP-PEG-Lys-FA polymer was immersed in 5 mL of the buffer solution and stirred at 150 rpm on magnetic stirrer at 37°C for 24 h. Polymer solutions were lyophilized and then molecular weight (Mw) and the Mw distribution of the degraded HBP-PEG-Lys-FA polymer in two different buffer solutions were determined by Gel Permeation Chromatography (Viscotek GPC/SEC system, Malvern, UK). Dimethylacetamide was used as mobile phase with a flow rate of 1 mL min⁻¹. Calibration was carried out using polystyrene calibration standards (Mw: from 400 Da to 30,000 Da; Sigma Aldrich, USA).

2.8. Preparation of empty and 5-Fu loaded HBP-PEG-Lys-FA nanoparticles

Empty and 5-Fu loaded nanoparticles were prepared using nanoprecipitation technique.^[36] One mL HBP-PEG-Lys-FA solution in DMF (10 mg/mL) was added dropwise into 9 mL PBS solution while magnetic stirring (600 rpm) at room temperature for 3 h to prepare the empty nanoparticles and then the resulting nanoparticle dispersion was dialyzed against PBS until DMF was completely removed. For the preparation of 5-Fu loaded nanoparticles, different amounts of 5-Fu were dissolved in the HBP-PEG-Lys-FA solution, and then the same procedure as mentioned above was followed.

2.9. Production yield of HBP-PEG-Lys-FA nanoparticles

The nanoparticle production yield was calculated by gravimetric analysis. 20 mL of nanoparticle dispersion were centrifuged (Optima XPN Ultracentrifuge, Beckman, USA) at 50,000 rpm for 1 h at 10°C and then particles were lyophilized at -40°C. The production yield was calculated as follows:

$$\text{Production yield(\%)} = \frac{\text{Weight of the nanoparticles}}{\text{Total solids(polymers + 5 - Fu)}} \quad (1)$$

2.10. Particle size and zeta potential of HBP-PEG-Lys-FA nanoparticles

The particle size and size distribution (Polydispersity index, PDI) were determined by photon correlation spectroscopy (Nano-ZS, Malvern Instruments, Malvern, UK) at 25°C. Three measurements were performed on each sample. Particle size was quoted as Z-average diameter for which the mean values and standard deviation calculated.

The zeta potential of nanoparticles was determined using an electrophoretic light-scattering technique (Zetasizer Nano-ZS, Malvern Instruments, Malvern, UK). The nanoparticles were dispersed in 10 mM potassium chloride solution. This dispersion was then added to the Zetasizer electrophoresis cell, the electrophoretic mobility was measured and the data converted to zeta potential values. Six measurements were performed on each sample and the mean values and standard deviations calculated.

2.11. Determination of actual drug content (AC) and encapsulation efficiency (EE) of HBP-PEG-Lys-FA nanoparticles

Nanoparticles were dissolved in ethanol and then 5-Fu amount in the solution was determined at 270 nm using UV-VIS spectrophotometer (T80 + UV-VIS Double Beam, PG Instruments, UK). All experiments were performed in triplicate. AC (mg/g) and EE (%) of nanoparticles were calculated using the following equations:

$$AC \left(\frac{\text{mg}}{\text{g}} \right) = \frac{M_{\text{act}}}{M_{\text{ms}}} \quad (2)$$

$$EE(\%) = \frac{M_{\text{act}}}{M_{\text{the}}} \quad (3)$$

Where M_{act} is the actual 5-Fu content in weighed quantity of nanoparticles, M_{ms} is the weighed quantity of powder of nanoparticles and M_{the} is the theoretical amount of 5-Fu in nanoparticles calculated from the quantity added in the process.

2.12. Serum stability studies

5-Fu loaded nanoparticles dispersed in both deionized water and PBS containing 5% FBS to determine the effect of serum to their physical stability. After 1 h incubation, the zeta potential, particle size and size distribution of nanoparticles were determined.

2.13. In vitro drug release studies

In vitro drug release studies were performed by the dialysis method.^[37] 10 mg of 5-Fu loaded nanoparticles were suspended in both 1 mL PBS solution and 1 mL pH 5.5 acetate buffer and transferred into the dialysis bags which were immersed in 9 mL of the same release medium (PBS or acetate buffer). At predetermined time intervals, 2 mL of the release medium from outside the dialysis bag were collected and subsequently 2 mL of fresh buffer solution were replaced. The amount of released 5-Fu was determined spectrophotometrically at 270 nm.

2.14. Cell culture studies

Human cervix epithelioid carcinoma (HeLa) cell was purchased from American Type Culture Collection (ATCC). The growth media used was DMEM supplemented with 10% (v/v) FBS, 100 IU mL⁻¹ penicillin and 100 mg mL⁻¹ streptomycin. The passage of the HeLa cells used was between 28 and 34. Cultures were maintained in 75 cm² culture flasks (Orange Scientific, Belgium) at 37°C in a humidified atmosphere with 5% CO₂. Media was changed every 2 days. When the cell monolayer reached 80–90% confluence, the HeLa cells were passaged using trypsin-EDTA solution (0.05% trypsin-EDTA) after washing twice with PBS. Cell viability was determined through staining with Trypan blue and cells were counted using hemocytometer. The suspended cells were seeded into 96-well plates at a density of 20.000 cells per well for cytotoxicity studies and at a density of 100.000 cells per well for cellular uptake studies. After seeding, the plates were incubated 24 h prior to the experiment.

2.15. Cytotoxicity studies

The *in vitro* cytotoxicity of empty and 5-Fu loaded nanoparticles was assessed by MTT test. Nanoparticles were diluted in the culture media (DMEM) to yield a concentration of 4 mg mL⁻¹ and then added to the cells to give a concentration range of 0.5–2 mg mL⁻¹. After incubation at 37°C, 5% CO₂, and 90% humidity for 24 and 48 h, the medium was removed by pipetting and 50 µL MTT in sterile PBS (2 µg mL⁻¹) was added to each well and then the plates were subjected to a further incubation of 2 h at 37°C in 5% CO₂ to allow formation of formazan crystals. Then, the unreduced MTT and medium was removed and the cells were washed with PBS. A 200 µL DMSO was then added to each well to dissolve the purple MTT formazan crystals and the plate was incubated at 37°C for 30 min. The absorbance of formazan products was measured at 570 nm using a microplate reader (Fluoroskan Ascent FL, ThermoFisher Scientific, USA). Empty nanoparticles were used as control group.

2.16. Cellular uptake of nanoparticles

HeLa cells were cultured in 4-well plates at a density of 100.000 cells per well and incubated until they formed a confluent monolayer. Upon reaching confluence, the culture medium was replaced with 500 µL DMEM with [FA(+)] or without [FA(-)] 1 mM sodium folate. After 1 h incubation, the culture medium was replaced with 500 µL DMEM containing calcein loaded nanoparticles (0.5 mg mL⁻¹) which were prepared using same method described in Section 2.8 by replacing 5-Fu with calcein. After incubation for 10 min, 30 min, 1 h and 4 h, the cells were gently washed with PBS and then observed under fluorescence microscope (IX71, Olympus, USA).

2.17. Receptor specificity of nanoparticles

Receptor specificity of the calcein loaded nanoparticles on HeLa cells was evaluated using flow cytometry. First, cells were

seeded into 35 mm petri dishes at a density of 300,000 cells per dish. When the cell monolayer reached 80–90% confluence, the cells were incubated with calcein loaded nanoparticles for 10 min, 30 min, 1 h and 4 h and then washed 3 times with PBS and trypsinized. Flow cytometry was performed with a BD Accuri™ C6 flow cytometer (BD Biosciences, USA).

3. Results and discussion

Nanoparticles sensitive to the pH gradients have made a great revolution in cancer therapy. They can be designed through various modifications such as changing their size, shape, chemical and physical properties, and so forth, in order to be able to target more efficiently the cancer cells.^[22] In this study, a novel 3rd generation hyperbranched polymer (HBP-PEG-Lys-FA) was structurally designed by our group and synthesized in house and then a pH-sensitive long-circulating nanoparticulate system was developed using same polymer for the selectively receptor mediated targeted delivery of anti-cancer agent, 5-Fu, to tumor cells without harming healthy cells.

3.1. Characterization of hyperbranched polymer

FA conjugated, DL-lysine modified, PEGylated, a novel 3rd generation hyperbranched HBP-PEG-Lys-FA polymer was synthesized in house. The general synthesis route of hyperbranched polymer is illustrated in Figure 1. In the first step, the 3rd generation aliphatic-polyester based hyperbranched polymer (HBP-OH) was prepared in the melt by an acid catalyzed polyesterification reaction starting from Bis-MPA as an AB₂ monomer and Et-TMP as a three-functional core. In the second step, HBP-OH was modified with carboxylic acid-terminated PEG to stabilize the nanoparticles in physiological conditions and to enhance their blood circulation time, then PEGylated polymer (HBP-PEG) was functionalized with positively charged DL-Lys, between –COOH groups of DL-Lys and -OH groups of HBP-PEG, to improve the interaction of positively charged groups of polymers and negatively charged cell membrane. In the last step, the obtained HBP-PEG-Lys was covalently conjugated to FA, targeting ligand,

through a carbodiimide mediated amide linkage, between the –NH₂ groups of HBP-PEG-Lys and the –COOH groups of FAs, to achieve the cellular uptake *via* folate receptor mediated endocytosis.

The synthesized polymers were characterized using ¹H-NMR ¹³C-NMR and FT-IR spectroscopy. The synthesis of the 3rd generation aliphatic-polyester based hyperbranched polymer (HBP-OH) was performed as described in Figure 2a. This synthesis route is simple and thus offers great opportunity for scaled-up preparation of hyperbranched polyesters. Reaction temperature is a significant parameter to minimize undesirable side reactions such as etherification and transesterification on preparation of dendrimer-like branched polyesters. For this reason, a relatively low esterification temperature (140°C) was chosen in this study.^[32] In addition, to increase the probability of unreacted acid groups reacted with the hydroxyl-terminated hyperbranched polymer and not with another free monomer, AB₂-type monomer was added in portions to the stirred reaction mixture.^[32]

The structure of the synthesized product was confirmed by FT-IR, ¹H NMR and ¹³C NMR analyses. Figure 2b shows the FT-IR spectrum of HBP-OH and the starting materials (Bis-MPA and Et-TMP). As seen in FT-IR spectra of the Et-TMP, the broad, small and sharp absorption bands or shoulders with various intensities at about 3100–3600 cm⁻¹, 1381 cm⁻¹, 877 cm⁻¹ and 777 cm⁻¹ regions were related to the stretching and deformation vibrations of the free OH groups of the CH₂OH groups. The absorption bands at about 1463 cm⁻¹ and 1060 cm⁻¹ were related to the deformation vibrations of the CH₂ bonds and the stretching vibrations of the C-O bonds of CH₂OH groups, respectively. In FT-IR spectra of the Bis-MPA, the small, broad and sharp absorption bands or shoulders with a variety of intensities at about 3364 cm⁻¹, 3223 cm⁻¹, 1309 cm⁻¹, 795 cm⁻¹ and 648 cm⁻¹ were related to the stretching and deformation vibrations of the free OH groups of the CH₂OH groups. The small absorption band at about 1464 cm⁻¹, 2948 cm⁻¹ and 2984 cm⁻¹ was related to the deformation vibrations, symmetric and asymmetric stretching vibrations of the CH₂ bonds of the CH₂OH groups, respectively. In the same spectra, the small

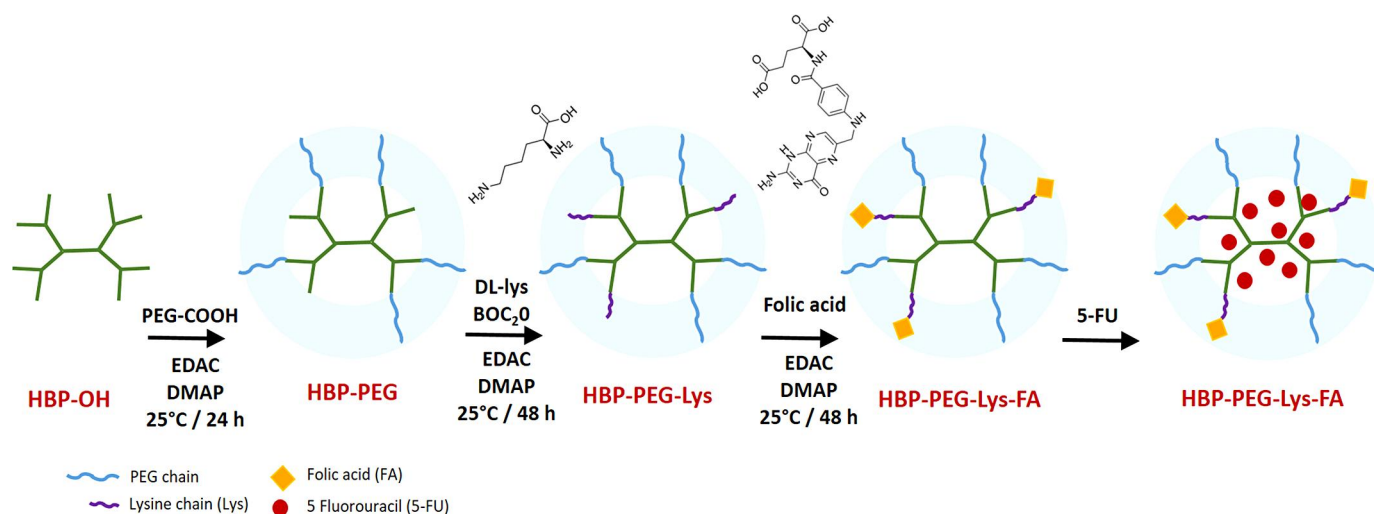


Figure 1. Schematic representation of the four-step synthesis of HBP-PEG-Lys-FA.

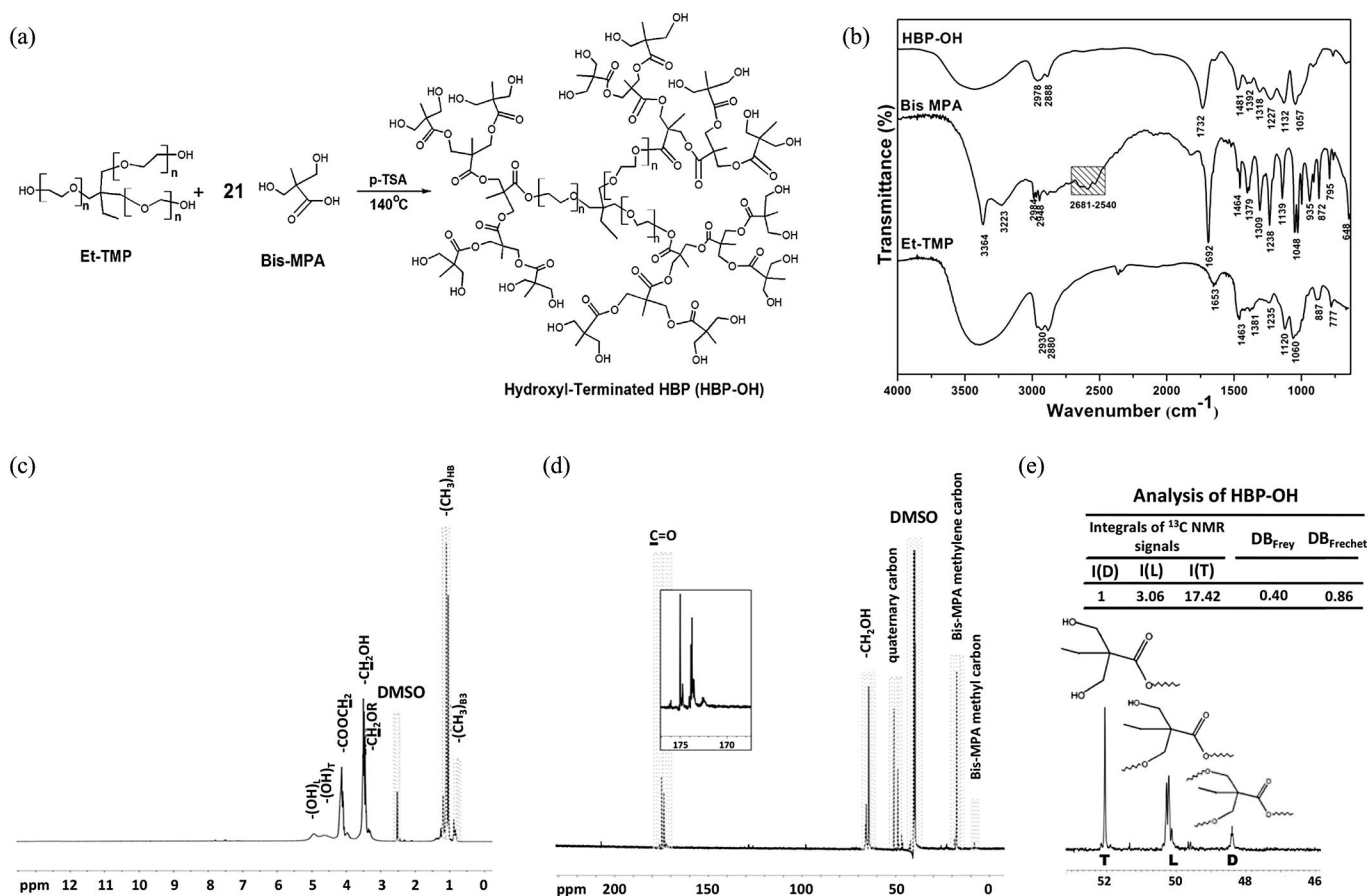


Figure 2. Structural properties of the 3rd generation hydroxyl-terminated hyperbranched polymer (HBP-OH); (a) HBP-OH polymer was synthesized by a pseudo-one-step procedure using Et-TMP as a core and bis-MPA as AB₂ type monomer. (b) FT-IR spectra of HBP-OH, (c) ¹H NMR spectra of HBP-OH, (d) ¹³C NMR spectra of HBP-OH, and (e) Magnification of the quaternary carbon region of the ¹³C NMR spectrum of HBP-OH, DB_{Frey} and DB_{Frechet} values determined from ¹³C NMR results according to Eq. (4) and (5).

and sharp absorption bands or shoulders with a variety of intensities at about 2681–2540 cm⁻¹, 1692 cm⁻¹ and 1139 cm⁻¹ regions were related to the stretching vibrations of the free OH groups of the COOH groups, the stretching vibrations of the C=O bonds of the COOH groups and the stretching vibrations of the C–O bonds of the COOH groups, respectively.^[38] However, the formation of the HBP-OH product was connected with the disappearance of the small and sharp absorption bands at about 2681–2540 cm⁻¹, 1692 cm⁻¹ and 1379 cm⁻¹ regions due to the stretching vibrations of the various bonds of the –COOH groups in the Bis-MPA molecule and the decrease or disappearance of the intensities of the absorption bands at about 3100–3600 cm⁻¹, 1463 cm⁻¹, 1381 cm⁻¹, 1060 cm⁻¹, 887 cm⁻¹ and 777 cm⁻¹ regions due to the stretching vibrations of the various bonds of the CH₂OH groups in the Et-TMP molecule. Also, formation of the ester structure of the HBP-OH product was confirmed with the appearance of a new small or sharp absorption band at 1732 cm⁻¹ depending on the structure of the core molecule and monomer due to the stretching vibrations of the C=O bonds of the aliphatic ester groups.^[38]

In the ¹H NMR spectra of HBP-OH (Figure 2c), the protons of the methyl group (–CH₃) in the terminal, linear and dendritic repeat units were observed at 1.02, 1.08, and 1.17 ppm, respectively. The signals of the methylene protons

(–CH₂–) were around at 3.48 ppm and 4.11 ppm. The signals from –(OH)_T and –(OH)_L protons resonated 4.6 and 4.9 ppm, respectively. The multi peaks appeared in ¹H NMR between 0.7–0.9 ppm contributed to the –CH₃ group of Et-TMP. The signals at around 3.36 ppm were due to the methylene protons of the ether groups (–CH₂OR) of Et-TMP as a result of etherification reaction between two intramolecular or intermolecular –OH groups. The signals of the unreacted –COOH groups protons of Bis-MPA (12–13 ppm) was not detected in the ¹H NMR spectra and therefore it was concluded that HBP-OH product was purified successfully.^[39]

In the ¹³C NMR spectra of HBP-OH (Figure 2d), the methyl (–CH₃) and methylene (–CH₂–) groups of Bis-MPA resonate at around 8.1 and 17.48 ppm, respectively.^[40] The other peak assignments are as follows: 47–51 ppm (quaternary carbons) and 172–176 ppm (carbonyl groups).^[40,41] Figure 2e shows the magnified quaternary carbon region of the ¹³C NMR spectra of the HBP-OH in DMSO. The signals of the quaternary carbon belonging to the dendritic, linear and terminal units are at 47.2, 49.03 and 51 ppm, respectively. To define and better understand the structure of hyperbranched polymers, Frechet and Frey introduced the average degree of branching, DB, for the hyperbranched polymers obtained from the polycondensation of AB₂ type monomers,

which can be calculated with the following the Frey and Frechet equations^[42,43]:

$$DB_{Frechet} = (D + T/D + L + T) \quad (4)$$

$$DB_{Frey} = (2D/(2D + L)) \quad (5)$$

D, L and T are integrals of completely reacted (dendritic), partially reacted (linear) and unreacted (terminal) fragments of the hyperbranched polymer, respectively. According to the Frechet definition, DB value for the perfect dendrimers should be 1, for the linear structures 0 and consequently, DB for the hyperbranched polymers is between 0 and 1. According to the later definition, Frey equation, DB value for the hyperbranched polymers should be between 0 and 0.5.^[41-43] $DB_{Frechet}$ and DB_{Frey} values determined from ¹³C NMR results according to the above equations are 0.86 and 0.40. Consequently, HBP-OH corresponds to the hyperbranched structure.

In the second step, HBP-OH was modified with a hydrophilic group, carboxylic acid-terminated PEG (PEG-COOH), to increase circulation time of nanoparticles in blood. Our first aim was to introduce a carboxylic acid functional group to the end of MPEG polymer chain to create a site for esterification with a hydroxyl group on HBP-OH. For this purpose, first, mPEG was functionalized through reaction with maleic anhydride^[33] to obtain PEG-COOH. The FT-IR spectra of mPEG and PEG-COOH are given in Figure 3a. The mPEG spectra showed the following absorption bands: 3100-3600 cm⁻¹ (free OH stretching vibrations of CH₂OH groups), 2890 cm⁻¹ (-CH₃ stretching vibration of CH₃-O-CH₂- groups), 1468 cm⁻¹ (-CH₃ deformation vibration of CH₃-O-CH₂- groups), 1148 cm⁻¹ (rocking vibration of CH₃-O-CH₂- groups), 1116 cm⁻¹, 1062 cm⁻¹ and 964 cm⁻¹ (C-O stretching vibration of CH₃-O-CH₂- groups). In the spectra of PEG-COOH, the new peak at 1742 cm⁻¹ is due to the presence of the ester bond, -CH=CH-CO-O(CH₂CH₂)_n- formation in the structure, suggesting a chemical bonding between the anhydride group of maleic anhydride and the hydroxyl group of PEG, while another peak around 1585 cm⁻¹ is due to the C=C stretching vibration of -CH=CH-CO-O(CH₂CH₂)_n- groups.^[44] All these results confirm the successful synthesis of the PEG-COOH. The following step was to introduce PEG-COOH segments into the HBP-OH macromolecule. HBP-OH was reacted with PEG-COOH at room temperature using DCC and DMAP as the catalysts. After the reaction was completed, the final product (HBP-PEG) was dialyzed against deionized water to remove the unreacted reactants. FT-IR spectrum of HBP-PEG is shown in Figure 3b. The formation of the HBP-PEG product was connected with the disappearance of the sharp absorption bands at about 1392 cm⁻¹ and 1057 cm⁻¹ existed in the spectra of HBP-OH due to the reaction between the methylol groups in HBP-OH and -COOH groups in the PEG-COOH. In addition, the appearance of peak at 1116 cm⁻¹ for C-O stretching vibration of CH₃-O-CH₂- groups confirms the pegylation reaction. To further confirm the formation of HBP-PEG, ¹H NMR spectrum was also recorded and is shown in Figure 3c. The peaks at about 3.50 ppm (a) and 3.32 ppm (a) for methylene groups and 3.24 ppm (b) for methyl groups were assigned to the protons

of methylene and methyl groups in the PEG segments, which confirms the synthesis of HBP-PEG.^[29]

Polymeric nanoparticles are functionalized with cationic groups, like amino groups, on their surface to enhance the cellular uptake because positively charged groups allows better uptake of the nanoparticles across the cell membrane.^[45] In the present study, DL-Lys was selected as the cationic moiety because DL-Lys is an aliphatic compound and essential amino acid of the human body^[46] and suitable for linking the backbone with the ligands due to the multiple amino groups.^[47] First, -NH₂ groups of DL-Lys were protected with (BOC)₂O under water-acetone catalyst-free conditions at room temperature,^[36] then -COOH groups of N-protected DL-Lys was activated with EDAC and reacted with -OH groups of HBP-PEG. The structure of the synthesized HBP-PEG-Lys product was confirmed by FT-IR and ¹H NMR analyses. Figure 3b shows the FT-IR spectra of HBP-PEG-Lys. Adsorption peaks at 2908 cm⁻¹ (-CH₂ stretching vibration of -CH₂NH₂ groups) and 1083 cm⁻¹ (-C-N- stretching vibration of -CH₂NH₂ groups) indicated the successful modification of HBP-PEG with DL-Lys. In addition, the ¹H NMR spectrum of HBP-PEG-Lys (Figure 3d) exhibited two new peaks at 2.61 ppm (methylene groups of DL-Lys, c) and 2.07 ppm (amine groups of DL-Lys, d),^[48] which confirms the synthesis of HBP-PEG-Lys.

In the last step, HBP-PEG-Lys was conjugated with a targeting agent for the enhancement of cellular uptake *via* receptor-mediated intracellular delivery mechanism. In this study, FA was chosen as the targeting agent because of its small size, non-immunogenicity, and high affinity to folate receptor which is expressed in low levels on healthy cells but highly expressed in various cancer cells.^[49-51] FA was covalently conjugated *via* its γ -carboxyl moiety to a polymer or drug. So, its binding affinity to folate receptor is not appreciably affected, and the receptor-mediated endocytosis proceeds unhindered.^[52,53] Molecular structure of the obtained product, HBP-PEG-Lys-FA, was verified by FT-IR and ¹H NMR analyses. FT-IR spectra of the HBP-PEG-Lys-FA conjugate (Figure 3b) displayed new small peak at 1402 cm⁻¹ corresponding to the deformation vibration of the phenyl ring of FA. The other peaks could not be quantified by FT-IR because these peaks were overlapped with the peaks of the HBP-PEG-Lys. To further confirm the formation of HBP-PEG-Lys-FA, ¹H NMR spectrum was also recorded and is shown in Figure 3e. The conjugation of folate to HBP-PEG-Lys was further supported by the appearance of weak signals at 6.7-8.7 ppm, which corresponded to the aromatic protons of FA.^[29]

3.2. pH dependent degradation studies

It is important to know the degradation behavior of the polymers under different physiological conditions to understand their fate within the body after administration and suitability for biomedical applications.^[54] They should be degraded to non-toxic small units and eliminated from the body. The accumulation of undegradable polymeric nanoparticles in the human blood circulation induce undesirable nanotoxicity by the time of progress.^[55] Polyester-based polymers are

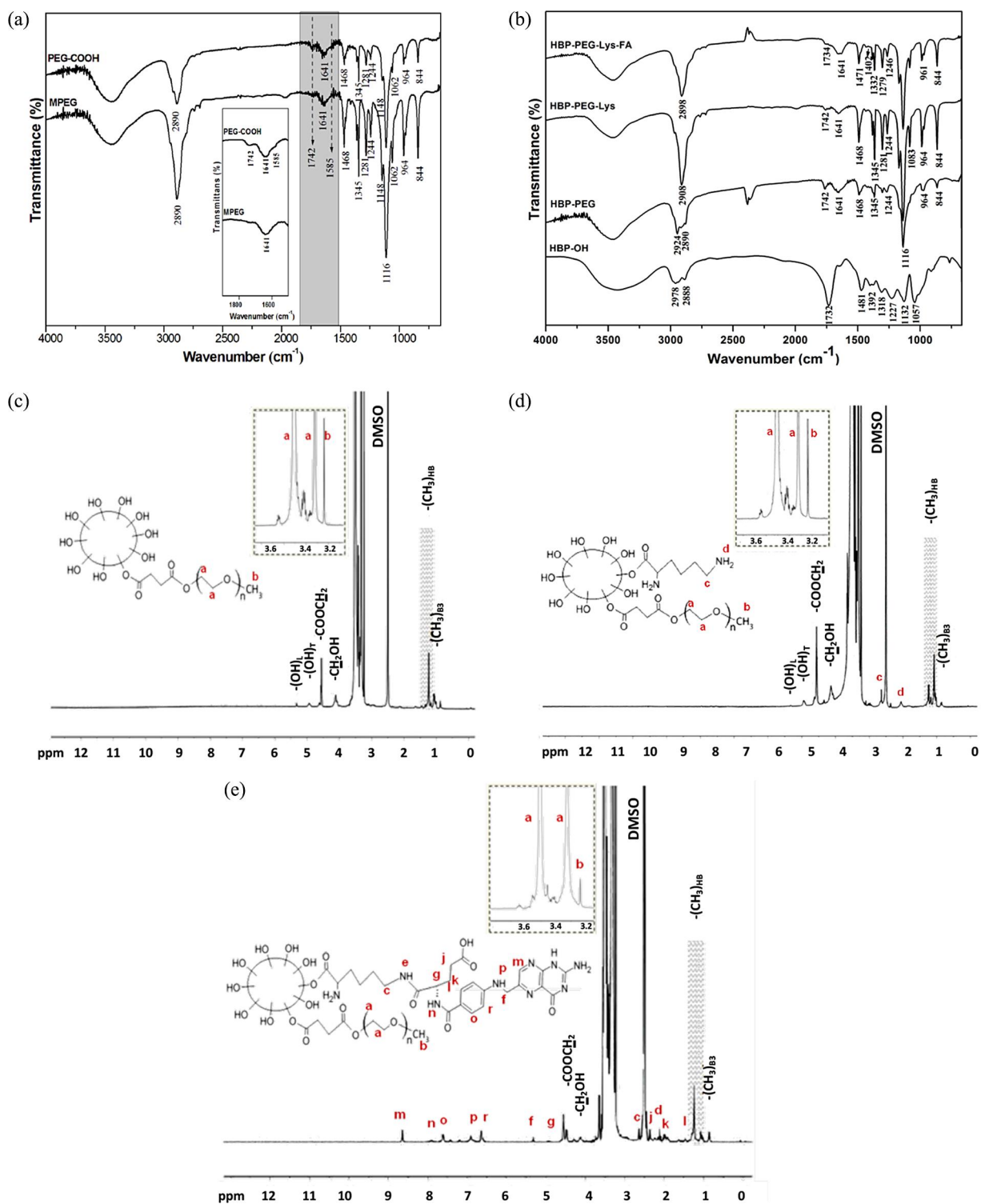


Figure 3. Structural properties of the functionalized HBPs; (a) FTIR spectra of PEG-COOH, (b) HBP-PEG, HBP-PEG-Lys, HBP-PEG-Lys-FA, (c) ¹H NMR spectra of HBP-PEG, (d) HBP-PEG-Lys and (e) HBP-PEG-Lys-FA.

attractive for the delivery of anticancer drugs due to their biodegradability in physiological conditions and the biocompatibility of the metabolites to the human body. It is probable that the cleavage of a backbone of the developed hyperbranched polymers can lead to its full degradation into low molecular weight monomers.^[55] Especially, hyperbranched polyester derivatives include ester bonds which degrade easily by a hydrolytic mechanism to small non-toxic units like

2,2-bis-(methyl)propionic acid and pentaerythritol.^[56] *In vitro* degradation behavior of hyperbranched HBP-PEG-Lys-FA polymer was investigated by changes in the polymer's molecular weight in pH 7.4 (to mimic the pH of blood) and 5.5 (to mimic the pH of late endosome) buffer solutions. As shown in Table 1, initial molecular weight (M_w) of HBP-PEG-Lys-FA polymer was around 11.456 Da. HBP-PEG-Lys-FA showed hydrolytic degradation and 63% and 72.6% of ester

Table 1. The degradation results of HBP-PEG-Lys-FA polymer in different simulated fluids (pH 7.4 and pH 5.5).

Sample	\bar{M}_w (g/mol)	PDI (Mw/ Mn)
HBP-PEG-Lys-FA	11456	2.0
HBP-PEG-Lys-FA ^a	4228	3.8
HBP-PEG-Lys-FA ^b	3140	4.1

^aDegradation of HBP-PEG-Lys-FA in pH 7.4 and ^bDegradation of HBP-PEG-Lys-FA in pH 5.5 buffer solution.

bonds in pH 7.4 and 5.5 buffer solutions were cleaved in 24 h, respectively. pH sensitive ester bonds on the structure significantly improved hydrolytic degradation of hyperbranched polymer in acidic media (endosomal pH 5.5). In a similar study, Lim et al. (2000) developed a non-toxic biodegradable aliphatic polyester based gene carrier, poly[α -(4-aminobutyl)-L-glycolic acid] (PAGA), containing a hydrolytically cleavable ester linkage and a positively-charged backbone. The synthesized polymer, PAGA, showed fast hydrolytic degradation that Mw decreased to 1/3 after only 100 min in pH 7.4.^[57] If this system is used for active targeting of cancer drugs, it would possibly degrade too fast in blood stream and will not be able to have sufficient time to reach the target area for delivery of therapeutic agents before degradation.^[58] As a result, our developed hyperbranched HBP-PEG-Lys-FA polymer, which has appropriate biodegradation characteristics in physiological conditions, is promising to prepare nanoparticles for active targeting the anti-cancer drugs to tumor cells.

3.3. Preparation of HBP-PEG-Lys-FA nanoparticles

An ideal nanoparticle system administered intravenously should ensure that the drug arrives and acts preferentially at the selected target. The size, size distribution and surface properties of particles are highly important factors to determine their *in vivo* fate. Particles in bloodstream are cleared according to their size and surface characteristics.^[59,60] Conventional nanoparticles larger than 30 nm are taken up by macrophages located in the liver and the spleen depends on opsonization by the mononuclear phagocytic system. A useful method for evading opsonization of nanoparticles is conjugation of hydrophilic polymers such as polyethylene glycol to the surface of the drug carrier.

On the other hand, particle size and surface properties play key roles in passive targeting and the cellular uptake of particles. The effective pore size in the endothelial lining of the blood vessels in most peripheral human tumors ranges from 200 nm to 600 nm^[61] and, generally, long-circulating nanoparticles smaller than 200 nm are capable of spontaneous accumulations at the tumor site via enhanced permeability and retention (EPR) effect as well as can be efficiently internalized through endocytosis by cancer cells.^[62]

Most of cancer cells over express the folate receptors and attachment of specific ligand, FA, on the surface of the particles also significantly improve their affinity to folate receptor which is expressed by most of cancer cells and uptake by receptor-mediated endocytosis.^[49–51]

In this study, we design and synthesized a new generation hyperbranched polymer (HBP-PEG-Lys-FA) which is PEGylated to improve the long circulating in blood stream,

modified with DL-lysine to enhance the interaction between particles and cancer cells, and conjugated a ligand, FA, to improve the receptor-mediated endocytosis by cancer cells. After structural characterization studies of hyperbranched polymer, the targeted nanoparticles containing a model anti-cancer drug, 5-Fu, smaller than 200 nm were developed and their effectiveness in cancer therapy were evaluated by *in vitro* cellular studies.

Numerous methods have been developed for fabrication of nanoparticles. These methods can be classified into two main categories according to whether the formulation requires a polymerization reaction or is achieved directly from the preformed polymer.^[63] Among these methods, nanoprecipitation (solvent displacement) method, which is simple and rapid technique, has the advantage of using preformed polymers as starting materials.^[37,40] This method allows the production of small nanoparticles with narrow size distribution and does not need stress conditions such as extended shearing/stirring rates, sonication and high temperature.^[36] Because of all these reasons, nanoprecipitation method was chosen to fabricate HBP-PEG-Lys-FA nanoparticles.

3.4. Characterization of 5-Fu loaded HBP-PEG-Lys-FA nanoparticles

The size and surface properties of nanoparticles are two important parameters for the determination of their *in vivo* fate.^[59,60] Keeping the particle size smaller than 200 nm and the zeta potential below 15 mV is important for internalization by endocytosis.^[64]

The potential of hyperbranched HBP-PEG-Lys-FA nanoparticles for selective targeting of 5-Fu, to folate receptor-positive cancer cells was investigated. First, 5-Fu loaded nanoparticles were prepared by nanoprecipitation technique^[36] at different polymer/drug ratios (1/1, 1/0.5, 1/0.25, 1/0.1 and 1/0.05, w/w) and then their entrapment efficiency and actual drug loading capacity were calculated. As shown in Figure 4c, entrapment efficiency increased with the increase in the polymer/drug mass ratio. This efficiency is very similar to that obtained through similar studies. For example, Nagarwal et al. (2011) developed 5-Fu loaded chitosan nanoparticles for ophthalmic delivery. Entrapment efficiency of the nanoparticles was enhanced from 8.12% to 34.32% with increasing of 5-Fu concentration.^[65] In another study, Xu et al. (2002), encapsulation efficiency of bovine serum albumin (BSA) particles dramatically increased around two times (26–47%) by increasing the initial BSA concentration.^[66] Besides, our results show that entrapment efficiency (0.68–35%) and actual drug loading (10.90–28.43%) of 5-Fu loaded nanoparticles was significantly changed depending on the mass ratio of polymer and drug. This may be explained by the elevated concentration gradient between polymer matrix and aqueous phase.^[67] Optimum drug loading (23.18 mg/g) was obtained at polymer/drug ratio of 1/0.25 (w/w), thus, the nanoparticles prepared at same ratio was chosen for further studies. The particle size and size distribution (PDI) of 5-Fu loaded (polymer/drug ratio of 1/0.25, w/w) nanoparticles were 177.7 ± 6.3 nm and 0.349, respectively (Figure 4a-b). Zeta potential value of

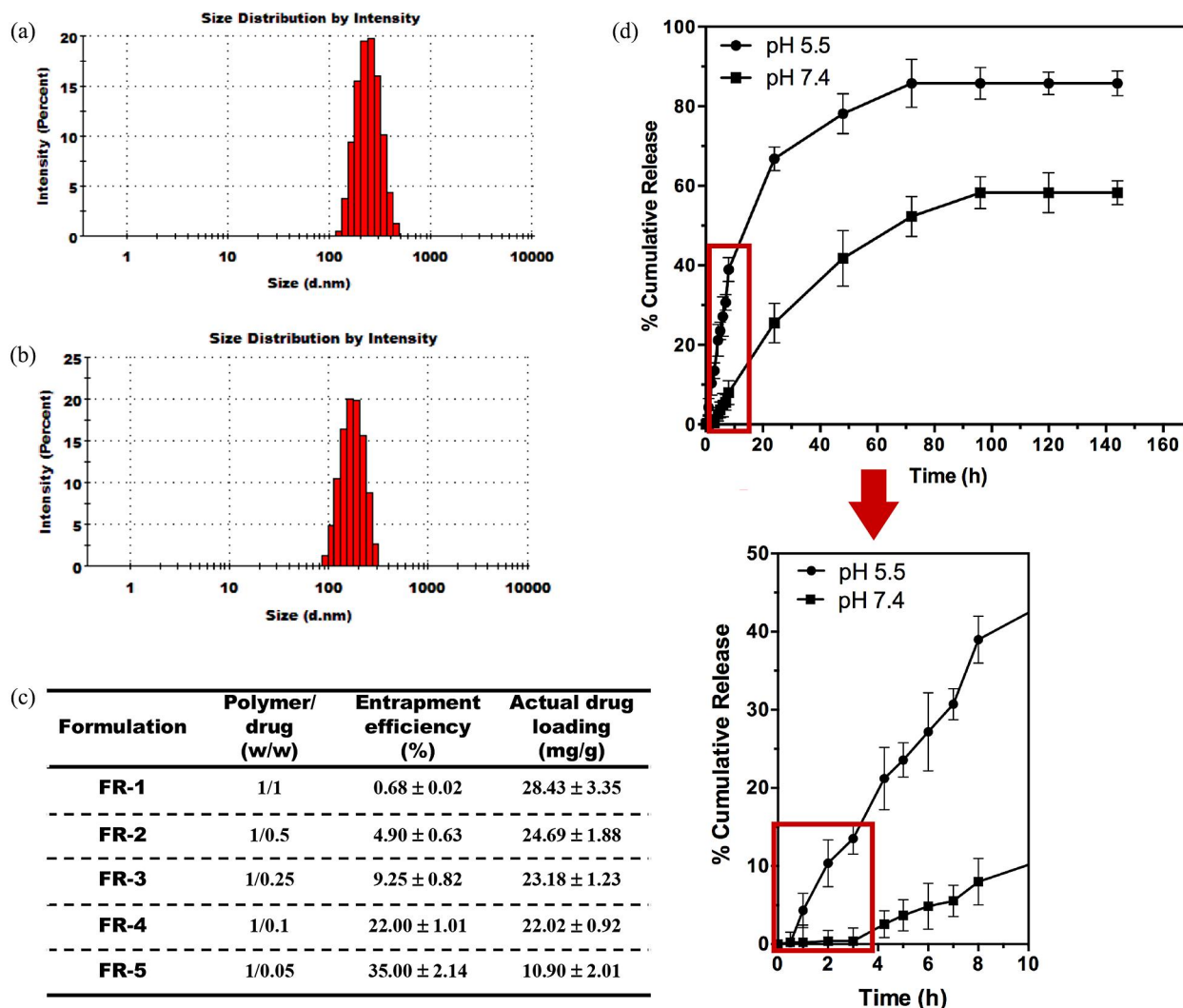


Figure 4. Particle size and drug release properties of 5-Fu loaded HBP-PEG-Lys-FA nanoparticles; (a) Particle size of empty HBP-PEG-Lys-FA nanoparticles (n = 6), (b) 5-Fu loaded HBP-PEG-Lys-FA nanoparticles (n = 6), (c) Effect of polymer/drug mass ratio on actual drug loading and entrapment efficiency of nanoparticles (n = 3), (d) In vitro drug release profile of 5-Fu from in different simulated fluids (n = 3).

nanoparticles was not significantly changed with incorporation of 5-Fu into the particles (-5.85 ± 0.88 mV) when compared that of empty ones (-8.15 ± 1.04 mV). Our findings are in line with the results of other groups.^[68,69]

The pH-sensitive nanoparticles increase the intracellular concentration of drugs in cancer cells and provide more effective cancer therapy, while preventing toxicity in healthy cells by decreasing the drug release in physiological pH of blood stream. Nanoparticles are enveloped by endosomes after their receptor-mediated endocytosis into the cells.^[70] The pH value in the interior of the endosome is acidic (pH 5.0-5.5) and the drug from the pH-sensitive nanoparticles can be released faster than conventional nanoparticles at low pH environment of the endosomes, and this improves the internal anti-cancer drug distribution in the cytosol. The *in vitro* cumulative % release of 5-Fu from nanoparticles at pH 7.4 and pH 5.5 is shown in Figure 4d. 5-Fu release from nanoparticles at pH 5.5 is faster than that of pH 7.4. Around 20% of 5-Fu was released within the first 4 h at pH 5.5, while only ~3% at pH 7.4. In 24 h, while drug release at pH 5.5 was 68%, around 2.6 times lower 5-Fu (26%) was released at pH 7.4 due to

pH sensitive nature of the synthesized polymer, HBP-PEG-Lys-FA, which degrades faster in acidic medium than physiological pH as confirmed by biodegradation studies. As seen in results of drug release studies, within the average delivering time of the nanoparticles to cancer cells (max. 3 h) indicated in the literature,^[29] while around 3% drug was released in pH value of blood stream (pH 7.4), the nanoparticles released up to 86% of the 5-Fu at endosomal pH value. Clearly, the reduced drug release rate from nanoparticles in the pH 7.4 and the significantly increased release in the pH 5.5 suggest that the nanoparticles developed would provide a major advantage on delivering of the drug efficiently into the cytosol for effective cancer therapy.^[71]

3.5. Serum stability of HBP-PEG-Lys-FA nanoparticles

Serum stability is an important key parameter as it determines the potency of nanoparticles to deliver the encapsulated drug in the structure safely to the targeted site and provides valuable prediction of nanoparticles behavior *in vivo*. Conventional nanoparticles can be quickly interacted with serum proteins

Table 2. Serum stability of HBP-PEG-Lys-FA nanoparticles (n = 3).

Sample	Nanoparticle suspension in the absence of FBS		Nanoparticle suspension in the presence of 5% (v/v) FBS	
	Z-average diameter (nm \pm SD)	PDI	Z-average diameter (nm \pm SD)	PDI
HBP-PEG-Lys-FA ^a	148.3 \pm 9.5	0.412	370.17 \pm 18.3	0.868
HBP-PEG-Lys-FA ^b	282.6 \pm 2.4	0.012	248.0 \pm 2.7	0.240

^aDispersion medium of nanoparticles is distilled water and ^bDispersion medium of nanoparticles is pH 7.4 PBS.

as soon as the nanoparticles get into the blood and form aggregates resulting in large particle size and broad size distribution.^[49,72] *In vitro* serum stability of nanoparticles was assessed by adding FBS into the nanoparticle dispersion and monitoring particle aggregation within a fixed time. For this purpose, empty HBP-PEG-Lys-FA nanoparticle formulations (prepared in two different media: deionized distilled water and PBS) were treated with FBS and changes in particle size and size distribution were examined. As shown in Table 2, the mean particle size and PDI of the nanoparticles prepared in distilled water increased from 148.3 nm to 370.17 nm as well as PDI from 0.412 to 0.868 in the presence of FBS. On the other hand, particle size of nanoparticles prepared in PBS was not significantly changed (from 282.6 nm to 248.0 nm) but PDI value increased from 0.012 to 0.240 which both are in acceptable limits. The nanoparticles prepared in PBS showed more physical stability in the presence of serum than those in water.

3.6. *In vitro* cytotoxicity studies

Biocompatibility of polymers used in drug carriers and effectiveness of drug loaded particles at target are major issues in developing drug delivery systems. In order to determine the biocompatibility of drug carriers prepared with hyperbranched polymer synthesized and the efficiency/effective dose of 5-Fu loaded nanoparticles on cancer cells, MTT assay, the most used assay to test the cytotoxicity of carries, was performed using HeLa cell line, derived from cervical cancer cells for use in cancer research, expressing folate receptors. Cytotoxic effect was evaluated as a function of nanoparticle concentration (0.5, 1, and 2 mg mL⁻¹) and the incubation time (6 and 24 h) to define dose-response and time-exposition effects, respectively. Sodium dodecyl sulfate (SDS) which is highly toxic to the cells^[73] was used as the positive control

and cells with no treatment as a negative control in cytotoxicity studies. As shown in Figure 5a, while empty nanoparticles were found to be less toxic to HeLa cells after 6 h incubation, 5-Fu loaded ones exhibited high cytotoxicity at same time. While an increase in drug loaded nanoparticle concentration from 0.5 to 2 mg mL⁻¹ reduced the cell viability dramatically from 45.05% to 6.63%, the reduction in cell viability for empty HBP-PEG-Lys-FA nanoparticles (from 97.02% to 43.99%) was significantly less. Incorporation of 5-Fu in hyperbranched HBP-PEG-Lys-FA nanoparticles strongly enhanced the cytotoxicity against HeLa cells.

Dendrimers and hyperbranched polymers bearing -NH₂ termini display concentration and usually generation dependent cytotoxicity. For example, polyamidoamine (PAMAM) dendrimers caused a decrease in cell (V79 Chinese hamster lung fibroblast) viability. The concentration producing 90% cell death was 7 ng/mL for generation 3 and 280 μ g/mL for generation 5.^[74] pH-sensitive HBP-PEG-Lys-FA polymer synthesized by our group (IC₅₀ \geq 1.78 mg/mL, calculated from Figure 5a) is significantly much less toxic than the pH-sensitive dendritic drug carriers such as PAMAM,^[74,75] polyethyleneimine (IC₅₀ = \sim 30 μ g/mL, in COS-7 cells) and poly(2-(dimethylamino)ethyl methacrylate) (IC₅₀ = \sim 40 μ g/mL, in COS-7 cells).^[76] Cytotoxicity of both empty and 5-Fu loaded nanoparticles after 24 h incubation was not significantly changed when compared to that of same particles after 6 h incubation (Figure 5b).

3.7. Cellular uptake studies using HeLa cells

The uptake of nanoparticles by cancer cells is critically important to be successful in cancer treatment without harming normal cells. A number of tumor cells including HeLa cells over express the folate receptors on their surface^[71]

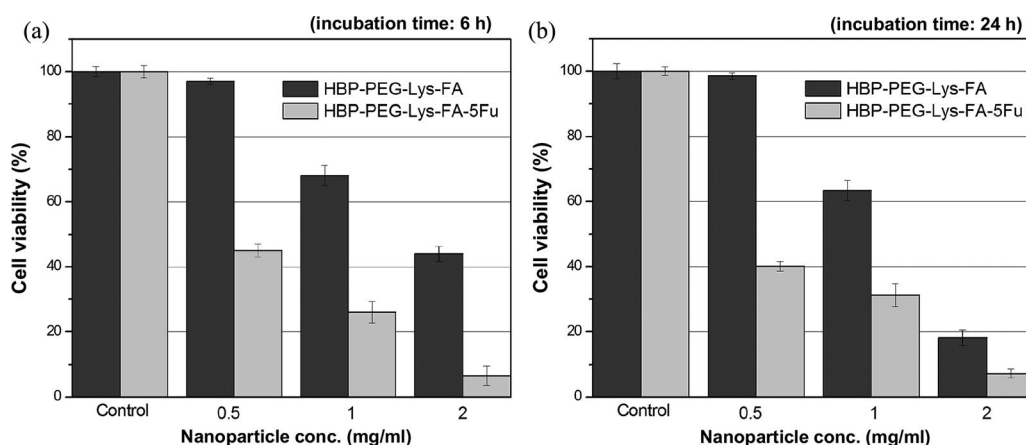


Figure 5. Cell viability of HBP-PEG-Lys-FA nanoparticles; Cytotoxicity of HBP-PEG-Lys-FA and HBP-PEG-Lys-FA-5Fu formulations after 6 h (a) and 24 h (b) incubation times on HeLa cells. The concentrations of the HBP-PEG-Lys-FA nanoparticles were 0.5, 1 and 2 mg/mL. (mean \pm SD, n = 3).

and particles containing FA on their structure are able to attach on the surface of cancer cells by lock and key mechanism.

In this study, the cellular uptake of calcein loaded HBP-PEG-Lys-FA nanoparticles by HeLa cells *via* the folate receptor mediated pathway were investigated by visualizing the dye up to 4 h using fluorescence microscopy. As seen in Figure 6a, green fluorescence in high intensity observed in the images proved that the nanoparticles entered into the HeLa cells *via* endocytosis. But, to confirm the receptor specificity of cellular uptake, folate receptors on cell membrane were blocked or drastically reduced by incubation of HeLa cells for 1 h with sodium folate prior to treatment with the nanoparticles (Figure 6b).^[77,78] Thus, sodium folate treated cells served as a model of healthy cells.^[79] As seen in Figure 6a and 6b, when the folate receptors blocked with free FA, much weaker green fluorescence is observed which proves that the calcein loaded nanoparticles barely internalized into the folate receptors blocked HeLa cells compared with cells over-expressed folate receptors. Consequently, the inhibition of uptake by free FA demonstrated that HBP-PEG-Lys-FA nanoparticles' uptake is mainly mediated by the folate receptor. In studies of Zhang et al. (2009) and Hajdu et al. (2014), the FA conjugated nanoparticles were significantly more internalized in HeLa cells untreated with free FA than in treated ones, proving receptor-mediated endocytosis,^[79,80] similar to our findings. The results interpreted in the light of other informations indicated that the developed nanoparticular drug carrier system would provide a major advantage for effective drug delivery to the cytosol of the targeted cancer cell.

3.8. Receptor specificity of HBP-PEG-Lys-FA nanoparticles

Nanoparticles' internalization in the HeLa cells was easily observed by fluorescence microscopy. Nevertheless, this method does not show the quantitative amount of particles inside the cells.^[77] Therefore, to achieve better understanding of receptor specificity and endocytosis, flow cytometry studies as a function of time were carried out. As shown in Figure 7,

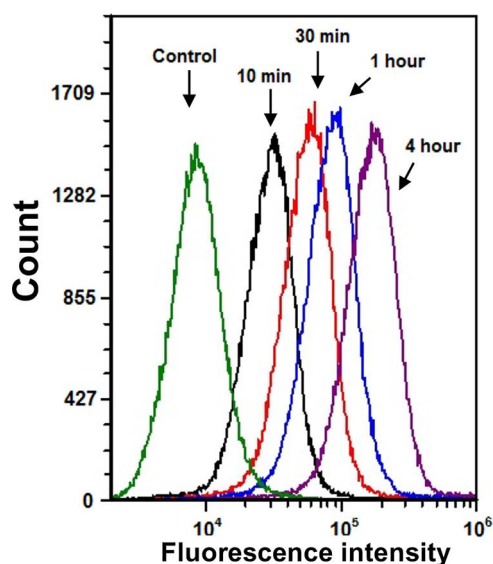


Figure 7. Flow cytometry histogram profiles of HeLa cells that were incubated with calcein-loaded HBP-PEG-Lys-FA nanoparticles for 10 min, 30 min, 1 h and 4 h. (nanoparticle concentration: 0.5 mg/mL).

HeLa cells without any treatment were used as a negative control and showed only the auto-fluorescence. A significant increasing fluorescence with augmenting incubation time of calcein loaded targeted HBP-PEG-Lys-FA nanoparticles with HeLa cells from 10 min to 4 h was observed, indicating receptor binding and internalization of the nanoparticles by folate-receptor mediated endocytosis as a function of time (Figure 7).

In similar studies, nanoparticles were conjugated with FA for the highly selective binding and internalization by the folate receptor-mediated endocytosis pathway. Alvarez-Berrios et al. (2016) evaluated the targeting abilities of FA conjugated mesoporous silica nanoparticles in HeLa cells using flow cytometry. The cells were exposed with FA conjugated nanoparticles for 6 h and the results clearly showed that the nanoparticles were internalized by the folate receptor-mediated endocytosis pathway.^[81] Dong et al. (2015) developed FA conjugated, PEGylated nanodiamond based

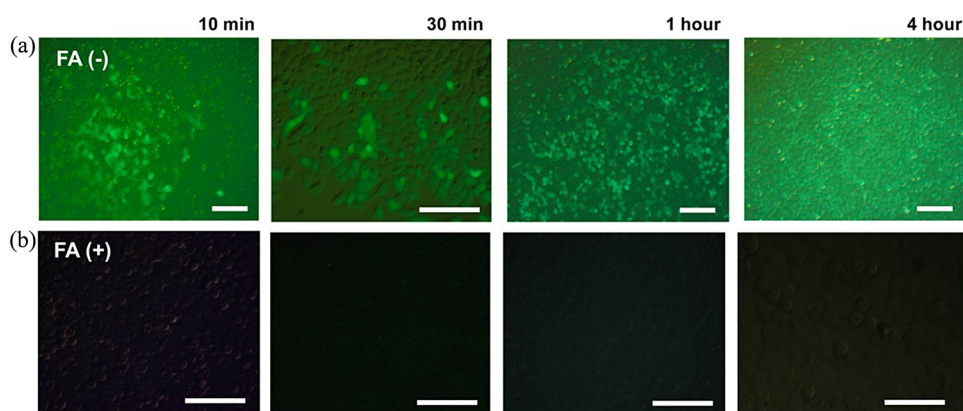


Figure 6. Cellular uptake and cell targeting properties of HBP-PEG-Lys-FA nanoparticles. Fluorescent microscopy images of (a) FA(-) HeLa cells and (b) FA(+) HeLa cells incubating for 10 min, 30 min, 1 h and 4 h with calcein-loaded HBP-PEG-Lys-FA nanoparticles (nanoparticle concentration: 0.5 mg/mL, scale bar: 200 μ m).

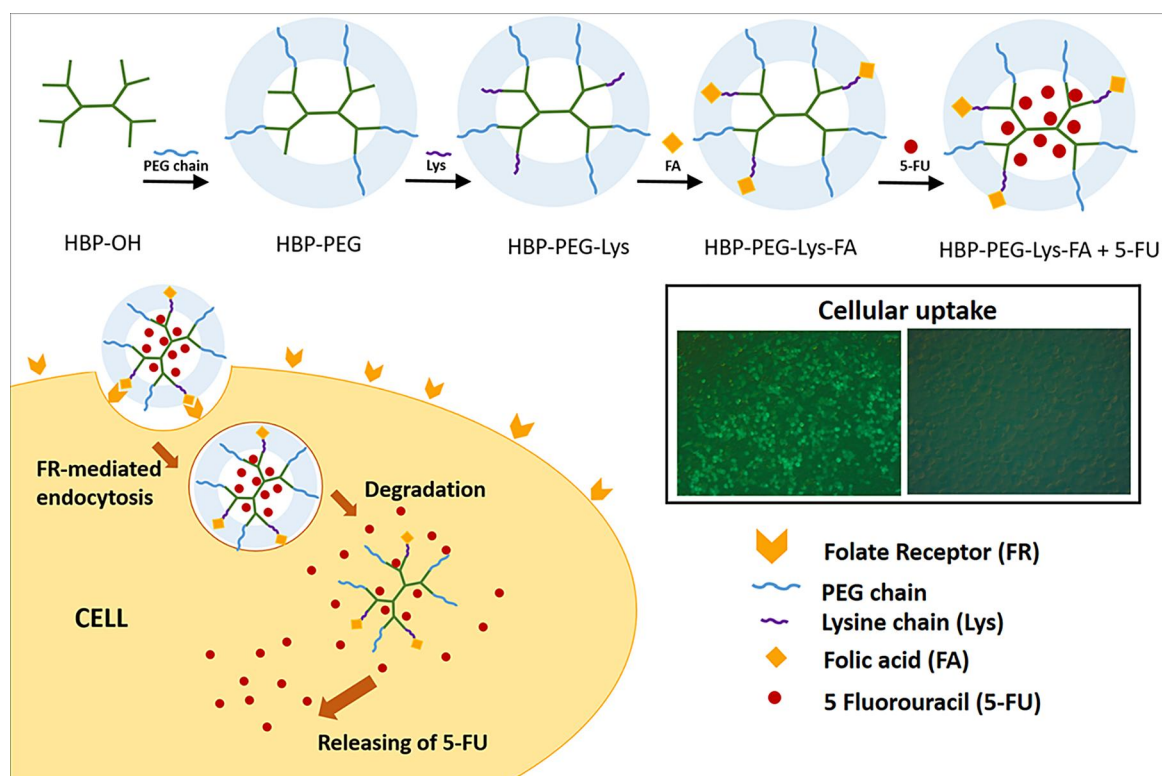


Figure 8. Releasing of 5-FU from the HBP-PEG-Lys-FA nanoparticles.

nanocarriers. HEK293 (low expressed folate receptors), HepG2 and HeLa (over expressed folate receptors) cells were used which have different amount of folate receptor expression level on their surface to evaluate targeting function of these nanoparticles. From the results of the flow cytometry analysis, it was understood that folate receptors played an important role in the endocytosis of nanoparticles.^[82] Consequently, regarding to similar studies, FA can be successfully used as a targeting ligand to enhance the intracellular accumulation of HBP-PEG-Lys-FA nanoparticles. Uptaking and releasing mechanism of the 5-Fu from the nanoparticles, which were designed in this study, was schematically presented in Figure 8.

4. Conclusions

In this study, it was developed a novel 5-Fu loaded pH sensitive targeted nanoparticulate system based on FA conjugated, DL-lysine modified, PEGylated, the 3rd generation hyper-branched polymer (HBP-PEG-Lys-FA) for receptor-mediated cancer treatment. Targeted HBP-PEG-Lys-FA nanoparticles were specifically attached to the surface receptors of cancer cells by means of targeting ligands and taken up into the cells by folate receptor-mediated endocytosis. 5-Fu release from nanoparticles at endosomal conditions at pH = 5.5 was significantly faster than that of physiologic conditions of blood stream at pH = 7.4. It was concluded that the nanoparticles developed can provide a major advantage on delivering of the drug efficiently into the cytosol for effective cancer therapy. Further studies are planned in the future to investigate

the efficacy of 5-Fu loaded HBP-PEG-Lys-FA nanoparticles on cancer therapy *in vivo*.

Acknowledgements

The authors wish to thank Assoc. Prof. Dr. Kamber Demir and DVM Selin Yağcıoğlu from the Department of Reproduction & Artificial Insemination at Istanbul University for their help with fluorescence microscope and flow cytometry studies. We also wish to thank Dr. Hande Tekarslan from the Department of Pharmaceutical Technology at Istanbul University for experimental assistance with regard to cell culture studies.

Funding

This work was supported by a grant of the Scientific Research Projects Coordination Unit of Istanbul University, project number 15349.

References

- [1] Nobs, L.; Buchegger, F.; Gurny, R.; Allémann, E. Biodegradable Nanoparticles for Direct or Two-Step Tumor Immunotargeting. *Bioconjugate Chem.* **2006**, *17*(1), 139–145. DOI: [10.1021/bc050137k](https://doi.org/10.1021/bc050137k).
- [2] Rosenholm, J.-M.; Sahlgren, C.; Lindén, M. Towards Multifunctional, Targeted Drug Delivery Systems Using Mesoporous Silica Nanoparticles—Opportunities & Challenges. *Nanoscale* **2010**, *2*(10), 1870–1883. DOI: [10.1039/c0nr00156b](https://doi.org/10.1039/c0nr00156b).
- [3] Gheybi, H.; Adeli, M. Supramolecular Anticancer Drug Delivery Systems Based on Linear-Dendritic Copolymers. *Polym. Chem.* **2015**, *6*(14), 2580–2615. DOI: [10.1039/C4PY01437E](https://doi.org/10.1039/C4PY01437E).
- [4] Byrne, J.-D.; Betancourt, T.; Brannon-Peppas, L. Active Targeting Schemes for Nanoparticle Systems in Cancer Therapeutics. *Adv. Drug Delivery Rev.* **2008**, *60*(15), 1615–1626. DOI: [10.1016/j.addr.2008.08.005](https://doi.org/10.1016/j.addr.2008.08.005).

- [5] Brannon-Peppas, L.; Blanchette, J.-O. Nanoparticle and Targeted Systems for Cancer Therapy. *Adv. Drug Delivery Rev.* **2012**, *64*, 206–212. DOI: [10.1016/j.addr.2012.09.033](https://doi.org/10.1016/j.addr.2012.09.033).
- [6] Yokoyama, M. Drug Targeting with Nano-Sized Carrier Systems. *J. Artif. Organs.* **2005**, *8*(2), 77–84. DOI: [10.1007/s10047-005-0285-0](https://doi.org/10.1007/s10047-005-0285-0).
- [7] Sethuraman, V.-A.; Bae, Y.-H. TAT Peptide-Based Micelle System for Potential Active Targeting of Anti-Cancer Agents to Acidic Solid Tumors. *J. Controlled Release.* **2007**, *118*(2), 216–224. DOI: [10.1016/j.jconrel.2006.12.008](https://doi.org/10.1016/j.jconrel.2006.12.008).
- [8] Wu, G.; Mikhailovsky, A.; Khant, H.-A.; Fu, C.; Chiu, W.; Zasadzinski, J.-A. Remotely Triggered Liposome Release by Near-Infrared Light Absorption via Hollow Gold Nanoshells. *J. Am. Chem. Soc.* **2008**, *130*(26), 8175–8177. DOI: [10.1021/ja802656d](https://doi.org/10.1021/ja802656d).
- [9] Singh, R.; Lillard, J.-W. Nanoparticle-Based Targeted Drug Delivery. *Exp. Mol. Pathol.* **2009**, *86*(3), 215–223. DOI: [10.1016/j.yexmp.2008.12.004](https://doi.org/10.1016/j.yexmp.2008.12.004).
- [10] Ray, A.; Larson, N.; Pike, D.-B.; Gruner, M.; Naik, S.; Bauer, H.; Ghandehari, H. Comparison of Active and Passive Targeting of Docetaxel for Prostate Cancer Therapy by HPMA Copolymer–RGDfK Conjugates. *Mol. Pharmaceutics.* **2011**, *8*(4), 1090–1099. DOI: [10.1021/mp100402n](https://doi.org/10.1021/mp100402n).
- [11] Avvakumova, S.; Colombo, M.; Tortora, P.; Prosperi, D. Biotechnological Approaches toward Nanoparticle Biofunctionalization. *Trends Biotechnol.* **2014**, *32*(1), 11–20. DOI: [10.1016/j.tibtech.2013.09.006](https://doi.org/10.1016/j.tibtech.2013.09.006).
- [12] Romberg, B.; Hennink, W.-E.; Storm, G. Sheddable Coatings for Long-Circulating Nanoparticles. *Pharm. Res.* **2008**, *25*(1), 55–71. DOI: [10.1007/s11095-007-9348-7](https://doi.org/10.1007/s11095-007-9348-7).
- [13] Moghimi, S.-M.; Hunter, A.-C.; Murray, J.-C. Long-Circulating and Target-Specific Nanoparticles: Theory to Practice. *Pharmacol. Rev.* **2001**, *53*(2), 283–318.
- [14] Chambers, E.; Mitragotri, S. Long Circulating Nanoparticles via Adhesion on Red Blood Cells: Mechanism and Extended Circulation. *Exp. Biol. Med.* **2007**, *232*(7), 958–966. DOI: [10.3181/00379727-232-2320958](https://doi.org/10.3181/00379727-232-2320958).
- [15] Gabizon, A.; Goren, D.; Horowitz, A.-T.; Tzemach, D.; Lossos, A.; Siegal, T. Long-Circulating Liposomes for Drug Delivery in Cancer Therapy: A Review of Biodistribution Studies in Tumor-Bearing Animals. *Adv. Drug Delivery Rev.* **1997**, *24*(2), 337–344. DOI: [10.1016/S0169-409X\(96\)00476-0](https://doi.org/10.1016/S0169-409X(96)00476-0).
- [16] Kommareddy, S.; Tiwari, S.-B.; Amiji, M.-M. Long-Circulating Polymeric Nanovectors for Tumor-Selective Gene Delivery. *Technol. Cancer Res. Treat.* **2005**, *4*(6), 615–625. DOI: [10.1177/153303460500400605](https://doi.org/10.1177/153303460500400605).
- [17] Kaur, S.; Prasad, C.; Balakrishnan, B.; Banerjee, R. Trigger Responsive Polymeric Nanocarriers for Cancer Therapy. *Biomater. Sci.* **2015**, *3*(7), 955–987. DOI: [10.1039/c5bm00002e](https://doi.org/10.1039/c5bm00002e).
- [18] Panyam, J.; Labhasetwar, V. Sustained Cytoplasmic Delivery of Drugs with Intracellular Receptors Using Biodegradable Nanoparticles. *Mol. Pharmaceutics.* **2004**, *1*(1), 77–84. DOI: [10.1021/mp034002c](https://doi.org/10.1021/mp034002c).
- [19] Xu, Z.-P.; Zeng, Q.-H.; Lu, G.-Q.; Yu, A.-B. Inorganic Nanoparticles as Carriers for Efficient Cellular Delivery. *Chem. Eng. Sci.* **2006**, *61*(3), 1027–1040. DOI: [10.1016/j.ces.2005.06.019](https://doi.org/10.1016/j.ces.2005.06.019).
- [20] Sutradhar, K.-B.; Amin, M.-L. Nanotechnology in Cancer Drug Delivery and Selective Targeting. *ISRN Nanotechnol.* **2014**, *2014*, 1–12. DOI: [10.1155/2014/939378](https://doi.org/10.1155/2014/939378).
- [21] Torchilin, V.-P.; Lukyanov, A.-N. Peptide and Protein Drug Delivery to and into Tumors: Challenges and Solutions. *Drug Discovery Today* **2003**, *8*(6), 259–266. DOI: [10.1016/S1359-6446\(03\)02623-0](https://doi.org/10.1016/S1359-6446(03)02623-0).
- [22] Rapoport, N. Physical Stimuli-Responsive Polymeric Micelles for Anti-Cancer Drug Delivery. *Prog. Polym. Sci.* **2007**, *32*(8), 962–990. DOI: [10.1016/j.progpolymsci.2007.05.009](https://doi.org/10.1016/j.progpolymsci.2007.05.009).
- [23] Kolhe, P.; Misra, E.; Kannan, R.-M.; Kannan, S.; Lieh-Lai, M. Drug Complexation, *In Vitro* Release and Cellular Entry of Dendrimers and Hyperbranched Polymers. *Int. J. Pharm.* **2003**, *259*(1), 143–160. DOI: [10.1016/S0378-5173\(03\)00225-4](https://doi.org/10.1016/S0378-5173(03)00225-4).
- [24] Zhang, H.; Zhao, C.; Cao, H.; Wang, G.; Song, L.; Niu, G.; Zhu, S. Hyperbranched Poly (Amine-Ester) Based Hydrogels for Controlled Multi-Drug Release in Combination Chemotherapy. *Biomaterials* **2010**, *31*(20), 5445–5454. DOI: [10.1016/j.biomaterials.2010.03.034](https://doi.org/10.1016/j.biomaterials.2010.03.034).
- [25] Rokicki, G.; Rakoczy, P.; Parzuchowski, P.; Sobiecki, M. Hyperbranched Aliphatic Polyethers Obtained from Environmentally Benign Monomer: Glycerol Carbonate. *Green Chem.* **2005**, *7*(7), 529–539. DOI: [10.1039/B501597A](https://doi.org/10.1039/B501597A).
- [26] Zhu, Z.; Kai, L.; Wang, Y. Synthesis and Applications of Hyperbranched Polyesters Preparation and Characterization of Crystalline Silver Nanoparticles. *Mater. Chem. Phys.* **2006**, *96*(2), 447–453. DOI: [10.1016/j.matchemphys.2005.07.067](https://doi.org/10.1016/j.matchemphys.2005.07.067).
- [27] Wang, T.; Li, M.; Gao, H.; Wu, Y. Nanoparticle Carriers Based on Copolymers of Poly (ϵ -Caprolactone) and Hyperbranched Polymers for Drug Delivery. *J. Colloid Interface Sci.* **2011**, *353*(1), 107–115. DOI: [10.1016/j.jcis.2010.09.053](https://doi.org/10.1016/j.jcis.2010.09.053).
- [28] Seiler, M. Hyperbranched Polymers: Phase Behavior and New Applications in the Field of Chemical Engineering. *Fluid Phase Equilib.* **2006**, *241*(1), 155–174. DOI: [10.1016/j.fluid.2005.12.042](https://doi.org/10.1016/j.fluid.2005.12.042).
- [29] Prabaharan, M.; Grailer, J.-J.; Pilla, S.; Steeber, D.-A.; Gong, S. Folate-Conjugated Amphiphilic Hyperbranched Block Copolymers Based on Boltorn[®] H40, Poly (L-Lactide) and Poly (Ethylene Glycol) for Tumor-Targeted Drug Delivery. *Biomaterials* **2009**, *30*(16), 3009–3019. DOI: [10.1016/j.biomaterials.2009.02.011](https://doi.org/10.1016/j.biomaterials.2009.02.011).
- [30] Shen, W.-C.; Ryser, H.-J. Conjugation of Poly-L-Lysine to Albumin and Horseradish Peroxidase: A Novel Method of Enhancing the Cellular Uptake of Proteins. *Proc. Natl. Acad. Sci. U. S. A.* **1978**, *75*(4), 1872–1876.
- [31] Kim, S.-H.; Jeong, J.-H.; Chun, K.-W.; Park, T.-G. Target-Specific Cellular Uptake of PLGA Nanoparticles Coated with Poly (L-Lysine)–Poly (Ethylene Glycol)–Folate Conjugate. *Langmuir* **2005**, *21*(19), 8852–8857. DOI: [10.1021/la0502084](https://doi.org/10.1021/la0502084).
- [32] Malmström, E.; Johansson, M.; Hult, A. Hyperbranched Aliphatic Polyesters. *Macromolecules* **1995**, *28*(5), 1698–1703. DOI: [10.1021/ma00109a049](https://doi.org/10.1021/ma00109a049).
- [33] Phan, Q.-T.; Le, M.-H.; Le, T.-T. H.; Tran, T. H. H.; Xuan, P.-N.; Ha, P.-T. Characteristics and Cytotoxicity of Folate-Modified Curcumin-Loaded PLA-PEG Micellar Nano Systems with Various PLA: PEG Ratios. *Int. J. Pharm.* **2016**, *507*(1), 32–40. DOI: [10.1016/j.ijpharm.2016.05.003](https://doi.org/10.1016/j.ijpharm.2016.05.003).
- [34] Cheraiet, Z.; Ouarna, S.; Hessainia, S.; Berredjem, M.; Aouf, N.-E. N-Tert-Butoxycarbonylation of Structurally Diverse Amines and Sulfamides under Water-Mediated Catalyst-Free Conditions. *ISRN Org. Chem.* **2012**, *2012*, 404235. DOI: [10.5402/2012/404235](https://doi.org/10.5402/2012/404235).
- [35] Han, G.; Tamaki, M.; Hruby, V.-J. Fast, Efficient and Selective Deprotection of the Tertbutoxycarbonyl (BOC) Group Using HCl/Dioxane (4m). *Chem. Biol. Drug Des.* **2001**, *58*(4), 338–341. DOI: [10.1034/j.1399-3011.2001.00935.x](https://doi.org/10.1034/j.1399-3011.2001.00935.x).
- [36] Bilati, U.; Allémann, E.; Doelker, E. Development of a Nanoprecipitation Method Intended for the Entrapment of Hydrophilic Drugs into Nanoparticles. *Eur. J. Pharm. Sci.* **2005**, *24*(1), 67–75. DOI: [10.1016/j.ejps.2004.09.011](https://doi.org/10.1016/j.ejps.2004.09.011).
- [37] Lee, E.-S.; Na, K.; Bae, Y.-H. Polymeric Micelle for Tumor pH and Folate-Mediated Targeting. *J. Controlled Release* **2003**, *91*(1), 103–113. DOI: [10.1016/S0168-3659\(03\)00239-6](https://doi.org/10.1016/S0168-3659(03)00239-6).
- [38] Socrates, G. *Infrared and Raman Characteristic Group Frequencies*; John Wiley & Sons: New York, 2001.
- [39] Žagar, E.; Žigon, M. Characterization of a Commercial Hyperbranched Aliphatic Polyester Based on 2, 2-Bis (Methylol) Propionic Acid. *Macromolecules* **2002**, *35*(27), 9913–9925. DOI: [10.1021/ma0210700](https://doi.org/10.1021/ma0210700).
- [40] Jena, K.-K.; Raju, K. V. S. N.; Prathab, B.; Aminabhavi, T.-M. Hyperbranched Polyesters: Synthesis, Characterization, and Molecular Simulations. *J. Phys. Chem. B* **2007**, *111*(30), 8801–8811. DOI: [10.1021/jp070513t](https://doi.org/10.1021/jp070513t).
- [41] Goswami, A.; Singh, A.-K. Hyperbranched Polyester Having Nitrogen Core: Synthesis and Applications as Metal Ion Extractant. *React. Funct. Polym.* **2004**, *61*(2), 255–263. DOI: [10.1016/j.reactfunctpolym.2004.06.006](https://doi.org/10.1016/j.reactfunctpolym.2004.06.006).
- [42] Hawker, C.-J.; Lee, R.; Fréchet, J. M. J. One-Step Synthesis of Hyperbranched Dendritic Polyesters. *J. Am. Chem. Soc.* **1991**, *113*(12), 4583–4588. DOI: [10.1021/ja00012a030](https://doi.org/10.1021/ja00012a030).

- [43] Jena, K.-K.; Narayan, R.; Raju, K. V. S. N. Hyperbranched Polyester Based on the Core+AB₂ Approach: Synthesis and Structural Investigation. *J. Appl. Polym. Sci.* **2010**, *118*(1), 280–290. DOI: 10.1002/app.32297.
- [44] Gupta, A.-K.; Wells, S. Surface-Modified Superparamagnetic Nanoparticles for Drug Delivery: Preparation, Characterization, and Cytotoxicity Studies. *IEEE Trans. Nanobioscience.* **2004**, *3*(1), 66–73. DOI: 10.1109/TNB.2003.820277.
- [45] Lorenz, M.-R.; Holzapfel, V.; Musyanovych, A.; Nothelfer, K.; Walthert, P.; Frank, H.; Mailänder, V. Uptake of Functionalized, Fluorescent-Labeled Polymeric Particles in Different Cell Lines and Stem Cells. *Biomaterials* **2006**, *27*(14), 2820–2828. DOI: 10.1016/j.biomaterials.2005.12.022.
- [46] Yu, W.; Liu, C.; Ye, J.; Zou, W.; Zhang, N.; Xu, W. Novel Cationic SLN Containing a Synthesized Single-Tailed Lipid as a Modifier for Gene Delivery. *Nanotechnology* **2009**, *20*(21), 215102. DOI: 10.1088/0957-4484/20/21/215102.
- [47] Papisov, M.-I.; Yurkovetskiy, A.; Syed, S.; Koshkina, N.; Yin, M.; Hiller, A.; Fischman, A. J. A. Systemic Route for Drug Loading to Lymphatic Phagocytes. *Mol. Pharmaceutics.* **2005**, *2*(1), 47–56. DOI: 10.1021/mp0499149.
- [48] Scholl, M.; Nguyen, T.-Q.; Bruchmann, B.; Klok, H.-A. The Thermal Polymerization of Amino Acids Revisited; Synthesis and Structural Characterization of Hyperbranched Polymers from L-Lysine. *J. Polym. Sci., Part A: Polym. Chem.* **2007**, *45*(23), 5494–5508. DOI: 10.1002/pola.22295.
- [49] Lee, R.-J.; Low, P.-S. Folate-Mediated Tumor Cell Targeting of Liposome-Entrapped Doxorubicin In Vitro. *Biochim. Biophys. Acta.* **1995**, *1233*(2), 134–144. DOI: 10.1016/0005-2736(94)00235-H.
- [50] Bi, X.; Shi, X.; Majoros, I.-J.; Shukla, R.; Baker, J.-R. Multifunctional Poly (Amidoamine) Dendrimer-Taxol Conjugates: Synthesis, Characterization and Stability. *J. Comput. Theor. Nanosci.* **2007**, *4*(6), 1179–1187. DOI: 10.1166/jctn.2007.2396.
- [51] Shakeri-Zadeh, A.; Ghasemifard, M.; Mansoori, G.-A. Structural and Optical Characterization of Folate-Conjugated Gold-Nanoparticles. *Phys. E.* **2010**, *42*(5), 1272–1280. DOI: 10.1016/j.physe.2009.10.039.
- [52] Sun, C.; Sze, R.; Zhang, M. Folic Acid PEG Conjugated Superparamagnetic Nanoparticles for Targeted Cellular Uptake and Detection by MRI. *J. Biomed. Mater. Res., Part A* **2006**, *78*(3), 550–557. DOI: 10.1002/jbm.a.30781.
- [53] Anirudhan, T.-S.; Anila, M.-M.; Franklin, S. Synthesis Characterization and Biological Evaluation of Alginate Nanoparticle for the Targeted Delivery of Curcumin. *Mater. Sci. Eng. C* **2017**, *78*, 1125–1134. DOI: 10.1016/j.msec.2017.04.116.
- [54] Çırpanlı, Y.; Allard, E.; Passirani, C.; Bilensoy, E.; Lemaire, L.; Çalıř, S.; Benoit, J.-P. Antitumoral Activity of Camptothecin-Loaded Nanoparticles in 9L Rat Glioma Model. *Int. J. Pharm.* **2011**, *403*(1), 201–206. DOI: 10.1016/j.ijpharm.2010.10.015.
- [55] Cheng, Y.; Zhao, L.; Li, Y.; Xu, T. Design of Biocompatible Dendrimers for Cancer Diagnosis and Therapy: Current Status and Future Perspectives. *Chem. Soc. Rev.* **2011**, *40*(5), 2673–2703. DOI: 10.1039/c0cs00097c.
- [56] Reul, R.; Nguyen, J.; Kissel, T. Amine-Modified Hyperbranched Polyesters as Non-Toxic, Biodegradable Gene Delivery Systems. *Biomaterials* **2009**, *30*(29), 5815–5824. DOI: 10.1016/j.biomaterials.2009.06.057.
- [57] Lim, Y.-B.; Han, S.-O.; Kong, H.-U.; Lee, Y.; Park, J.-S.; Jeong, B.; Kim, S.-W. Biodegradable Polyester, Poly [A-(4-Aminobutyl)-L-Glycolic Acid], as a Non-Toxic Gene Carrier. *Pharm. Res.* **2000**, *17*(7), 811–816. DOI: 10.1023/A:1007552007765.
- [58] Petersen, H.; Merdan, T.; Kunath, K.; Fischer, D.; Kissel, T. Poly (Ethylenimine-co-L-Lactamide-co-Succinamide): A Biodegradable Polyethylenimine Derivative with an Advantageous pH-Dependent Hydrolytic Degradation for Gene Delivery. *Bioconjugate Chem.* **2002**, *13*(4), 812–821. DOI: 10.1021/bc0255135.
- [59] Deng, C.; Chen, X.; Yu, H.; Sun, J.; Lu, T.; Jing, X. A Biodegradable Triblock Copolymer Poly (Ethylene Glycol)-b-Poly (L-Lactide)-b-Poly (L-Lysine): Synthesis, Self-Assembly, and RGD Peptide Modification. *Polymer* **2007**, *48*(1), 139–149. DOI: 10.1016/j.polymer.2006.10.046.
- [60] Kulkarni, S.-A.; Feng, S.-S. Effects of Particle Size and Surface Modification on Cellular Uptake and Biodistribution of Polymeric Nanoparticles for Drug Delivery. *Pharm. Res.* **2013**, *30*(10), 2512–2522. DOI: 10.1007/s11095-012-0958-3.
- [61] Torchilin, V.-P. Targeted Pharmaceutical Nanocarriers for Cancer Therapy and Imaging. *AAPS J.* **2007**, *9*(2), E128–E147. DOI: 10.1208/aapsj0902015.
- [62] Quignard, S.; Masse, S.; Coradin, T. Silica-Based Nanoparticles for Intracellular Drug Delivery, Fundamentals and Applications. In *Intracellular Delivery, Fundamentals and Applications*; Prokop, A., Ed.; Springer: New York, 2011; Part II, pp 333–361.
- [63] Reis, C.-P.; Neufeld, R.-J.; Ribeiro, A.-J.; Veiga, F. Nanoencapsulation I. Methods for Preparation of Drug-Loaded Polymeric Nanoparticles. *Nanomedicine: NBM* **2006**, *2*(1), 8–21. DOI: 10.1016/j.nano.2005.12.003.
- [64] Zauner, W.; Farrow, N.-A.; Haines, A.-M. In Vitro Uptake of Polystyrene Microspheres: Effect of Particle Size, Cell Line and Cell Density. *J. Controlled Release* **2001**, *71*(1), 39–51. DOI: 10.1016/S0168-3659(00)00358-8.
- [65] Nagarwal, R.-C.; Singh, P.-N.; Kant, S.; Maiti, P.; Pandit, J.-K. Chitosan Nanoparticles of 5-Fluorouracil for Ophthalmic Delivery: Characterization, In-Vitro and In-Vivo Study. *Chem. Pharm. Bull.* **2011**, *59*(2), 272–278. DOI: 10.1248/cpb.59.272.
- [66] Xu, Y.; Du, Y. Effect of Molecular Structure of Chitosan on Protein Delivery Properties of Chitosan Nanoparticles. *Int. J. Pharm.* **2003**, *250*(1), 215–226. DOI: 10.1016/S0378-5173(02)00548-3.
- [67] Dong, Y.; Feng, S.-S. Methoxy Poly (Ethylene Glycol)-Poly (Lactide) (MPEG-PLA) Nanoparticles for Controlled Delivery of Anticancer Drugs. *Biomaterials* **2004**, *25*(14), 2843–2849. DOI: 10.1016/j.biomaterials.2003.09.055.
- [68] Mccarron, P. A. U. L.; Woolfson, A.-D.; Keating, S.-M. Sustained Release of 5-Fluorouracil from Polymeric Nanoparticles. *J. Pharm. Pharmacol.* **2000**, *52*(12), 1451–1459. DOI: 10.1211/0022357001777658.
- [69] Kalra, A.-V.; Campbell, R.-B. Development of 5-FU and Doxorubicin-Loaded Cationic Liposomes Against Human Pancreatic Cancer: Implications for Tumor Vascular Targeting. *Pharm. Res.* **2006**, *23*(12), 2809–2817. DOI: 10.1007/s11095-006-9113-3.
- [70] Cho, K.; Wang, X.-U.; Nie, S.; Shin, D.-M. Therapeutic Nanoparticles for Drug Delivery in Cancer. *Clin. Cancer Res.* **2008**, *14*(5), 1310–1316. DOI: 10.1158/1078-0432.CCR-07-1441.
- [71] Shen, Z.; Li, Y.; Kohama, K.; Oneill, B.; Bi, J. Improved Drug Targeting of Cancer Cells by Utilizing Actively Targetable Folic Acid-Conjugated Albumin Nanospheres. *Pharmacol. Res.* **2011**, *63*(1), 51–58. DOI: 10.1016/j.phrs.2010.10.012.
- [72] Ruan, S.; Qian, J.; Shen, S.; Zhu, J.; Jiang, X.; He, Q.; Gao, H. A Simple One-Step Method to Prepare Fluorescent Carbon Dots and Their Potential Application in Non-Invasive Glioma Imaging. *Nanoscale* **2014**, *6*(17), 10040–10047. DOI: 10.1039/C4NR02657H.
- [73] Green, M.; Howes, P.; Berry, C.; Argyros, O.; Thanou, M. Simple Conjugated Polymer Nanoparticles as Biological Labels. *Proc. R. Soc. A* **2009**, *465*(2109), 2751–2759. DOI: 10.1098/rspa.2009.0181.
- [74] Duncan, R.; Izzo, L. Dendrimer Biocompatibility and Toxicity. *Adv. Drug Delivery Rev.* **2005**, *57*(15), 2215–2237. DOI: 10.1016/j.addr.2005.09.019.
- [75] Jevprasesphant, R.; Penny, J.; Jalal, R.; Attwood, D.; McKeown, N.-B.; D’emanuele, A. The Influence of Surface Modification on the Cytotoxicity of PAMAM Dendrimers. *Int. J. Pharm.* **2003**, *252*(1), 263–266. DOI: 10.1016/S0378-5173(02)00623-3.
- [76] Zhong, Z.; Song, Y.; Engbersen, J.-F.; Lok, M.-C.; Hennink, W.-E.; Feijen, J. A Versatile Family of Degradable Non-Viral Gene Carriers Based on Hyperbranched Poly (Ester Amine) s. *J. Controlled Release* **2005**, *109*(1), 317–329. DOI: 10.1016/j.jconrel.2005.06.022.
- [77] Zhang, X.; Meng, L.; Lu, Q.; Fei, Z.; Dyson, P.-J. Targeted Delivery and Controlled Release of Doxorubicin to Cancer Cells Using Modified Single Wall Carbon Nanotubes. *Biomaterials* **2009**, *30*(30), 6041–6047. DOI: 10.1016/j.biomaterials.2009.07.025.
- [78] Wang, Y.; Li, P.; Chen, L.; Gao, W.; Zeng, F.; Kong, L.-X. Targeted Delivery of 5-Fluorouracil to HT-29 Cells Using High Efficient

- Folic Acid-Conjugated Nanoparticles. *Drug Delivery* **2015**, 22(2), 191–198. DOI: [10.3109/10717544.2013.875603](https://doi.org/10.3109/10717544.2013.875603).
- [79] Hajdú, I.; Trencsényi, G.; Bodnár, M.; Emri, M.; Bánfalvi, G.; Sikula, J.; Márián, T.; Kollár, J.; Vámosi, G.; Borbély, J. Tumor-Specific Localization of Self-Assembled Nanoparticle PET/MR Modalities. *Anticancer Res.* **2014**, 34(1A), 49–60.
- [80] Zhang, B.; Li, Y.; Fang, C.-Y.; Chang, C.-C.; Chen, C.-S.; Chen, Y.-Y.; Chang, H.-C. Receptor-Mediated Cellular Uptake of Folate Conjugated Fluorescent Nanodiamonds: A Combined Ensemble and Single Particle Study. *Small* **2009**, 5(23), 2716–2721. DOI: [10.1002/smll.200900725](https://doi.org/10.1002/smll.200900725).
- [81] Alvarez-Berrios, M.-P.; Vivero-Escoto, J.-L. In Vitro Evaluation of Folic Acid-Conjugated Redox-Responsive Mesoporous Silica Nanoparticles for the Delivery of Cisplatin. *Int. J. Nanomed.* **2016**, 11, 6251. DOI: [10.2147/IJN.S118196](https://doi.org/10.2147/IJN.S118196).
- [82] Dong, Y.; Cao, R.; Li, Y.; Wang, Z.; Li, L.; Tian, L. Folate-Conjugated Nanodiamond for Tumor-Targeted Drug Delivery. *RSC Adv.* **2015**, 5(101), 82711–82716. DOI: [10.1039/C5RA12383F](https://doi.org/10.1039/C5RA12383F).